

NPS ARCHIVE
1964
BOSSART, E.



MASSACHUSETTS INSTITUTE OF TECHNOLOGY

AN INVESTIGATION OF THE SURFACE-TO-UNDERWATER FIRE CONTROL PROBLEM

by

Lieutenant Edmund Belfour Bossart, Jr.
United States Navy
May 1964

Master of Science Thesis

T-383

PREPARED AT

INSTRUMENTATION LABORATORY
MASSACHUSETTS INSTITUTE OF TECHNOLOGY
CAMBRIDGE 39, MASSACHUSETTS

Thesis
B726

**DUDLEY KNOX LIBRARY
NAVAL POSTGRADUATE SCHOOL
MONTEREY, CA 93943-5101**

AN INVESTIGATION OF
THE SURFACE-TO-UNDERWATER FIRE CONTROL PROBLEM

by

Lieutenant EDMUND BELFOUR BOSSART, JR. United States Navy
B.S., United States Naval Academy
(1955)

B.S.E.E., United States Naval Postgraduate School
(1963)

SUBMITTED IN PARTIAL FULFILLMENT
OF THE REQUIREMENTS FOR THE
DEGREE OF MASTER OF SCIENCE

at the

MASSACHUSETTS INSTITUTE OF TECHNOLOGY
May, 1964

AN INVESTIGATION OF
THE SURFACE-TO-UNDERWATER FIRE CONTROL PROBLEM

by

Lieutenant EDMUND BELFOUR BOSSART, JR. United States Navy

Submitted to the Department of Aeronautics and Astronautics
on 18 May 1964 in partial fulfillment of the requirements for the
degree of Master of Science.

ABSTRACT

This investigation is an extension of the work of Wrigley
and Hovorka in fire control to the problem of the thesis. Quanti-
ties peculiar to the underwater problem are defined, examined, and
illustrated when appropriate. Using these quantities and those
from the "above-water" problem that apply, the problem is formu-
lated. Two possible methods of solution are discussed and
compared.

Thesis Supervisor: Walter Wrigley, Sc.D.

Title: Professor of Instrumentation
and Astronautics

BUDLEY
NAVY
MONTEREY, CA 93940-41

ACKNOWLEDGEMENTS

The author wishes to thank the Bureau of Naval Weapons for sponsoring his three years of postgraduate education which have culminated in the presentation of this thesis. Special appreciation is due to Professor Walter Wrigley, who as thesis supervisor gave generously of his time in discussing the research and made many constructive suggestions. The typing of the manuscript was ably done by Joan D. Ginn.

The publication of this report is not a statement of the views or approval of the Bureau of Naval Weapons or the U. S. Navy of the United States. The conclusions contained therein. It is published only for the exchange and stimulation of ideas.

TABLE OF CONTENTS

<u>Chapter</u>		<u>Page</u>
I	Introduction	1
	1. The Advent of the Stand-Off ASW Weapon	1
	2. Previous Work in Fire Control	2
	3. Outline of Attack	2
II	Quantities Peculiar to the Underwater Fire Control Problem	3
	1. Introduction	3
	2. Splash Point	3
	3. The Water-Mass Coordinate Frame	4
	4. Transmission Time	5
	5. Line of Sight and Line of Position	5
	6. Target Velocity	7
	7. Sinking Time	7
	8. Future Range	7
	9. Offset Range and Future Line of Position	8
	10. Summary: the Determination of Splash Range	9
III	Formulation of the Problem	10
	1. Introduction: Miss-Producing Effects	10
	2. Corrections for Miss-Producing Effects	11
	3. Prediction Angle and the Prediction Angle Vector	12
	4. Lead	13
	5. Curvature Correction	15

<u>Chapter</u>	<u>Page</u>
III	6. Jump Correction 18
	7. Summary 18
IV	Solution of the Problem 25
	1. Introduction 25
	2. Information Rate 25
	3. Transformation of Target Information 26
	4. The Triangulation Method 26
	5. The Controlled Line Method 28
	6. A Simple Analysis of the Preceding Two Methods 32
	7. Summary 36
V	Summary and Conclusions 38
	1. Problems Caused by the Target's Being Underwater 38
	2. Methods for Solving the Surface-to-Underwater Fire Control Problem 39
	3. Suggestions for Further Work 39
<u>Derivation Summary</u>	
	3.1 21
<u>Figures</u> 41	
<u>Appendix</u>	
A	An Example of Target Information Transformation 53
<u>References</u> 57	

LIST OF FIGURES

<u>Figure</u>		<u>Page</u>
1.	Geometrical Features of the Splash Point	41
2.	Transmission Time	42
3.	The Relationship Between Line of Sight and Line of Position	42
4.	Sinking Time	43
5.	The Relationship of Future Range and Offset Range to Splash Range	44
6.	Center of Lethality	44
7.	Target Motion as a Miss-Producing Effect	45
8.	Curvature of the Trajectory as a Miss-Producing Effect	45
9.	Jump as a Miss-Producing Effect	46
10.	Geometrical Features of the Complete Problem	46
11.	Geometrical Features of Lead Angle	47
12.	Geometrical Features of Curvature Correction	48
13.	Geometrical Features of Jump Correction	48
14.	Information Rates in Electromagnetic and Sound Radiation	49
15.	Determination of \bar{V}_{Ta}	50
16.	The Geometrical Relationships Between the Line of Sight, the Tracking Line, and the Correction to the Tracking Line	51
17.	A Signal Modifier For Use With the Controlled Line Method	52
A-1	Axis Systems in Weapon Station Structure Angular Motion	56

CHAPTER I

INTRODUCTION

1.1 The Advent of the Stand-Off ASW Weapon

A common conception of surface ship antisubmarine warfare is the picture of a destroyer plunging through the seas, dropping depth charges and firing short-ranged hedgehogs at a somewhat elusive target. This is not true today and will be even less true in the future. According to Vice Admiral John W. Thach, USN, Commander Antisubmarine Warfare Force, U.S. Pacific Fleet in a recent article:

The new ASW destroyers will be very different from their predecessors. Their detection capability will be much longer ranged and sharper than it is today... Multi-purpose missile systems with accurate fire control to provide for early attack at long ranges will be forthcoming in the next decade... (1)

Thus the surface-to-underwater fire control problem is one of interest and its scope is changing rapidly. In the past, ASW ships little more than threw explosive rocks into the water when they thought they were about over the target. Even the throwing was slow and the time that elapsed between the order to throw and the throwing had to be taken into consideration. Such will not be the case in the future. Detection systems and weapons will permit a destroyer to engage his foe at long range.

(1) The numbers in parentheses refer to cited references in the Bibliography.

1.2 Previous Work in Fire Control

This thesis is based on the work done in fire control theory at the Massachusetts Institute of Technology by Walter Wrigley and John Hovorka. Their book Fire Control Principles⁽²⁾ separates the fire control problem from its solution and the principles from the actual systems. It deals with "above-water" fire control and assumes the use of electromagnetic radiation to obtain target information. This writer is aware of previous work, some classified, in the underwater fire control field, but as far as he has been able to determine, this thesis is the first work of its nature. It is an extension of the line of attack pursued by Wrigley and Hovorka to the surface-to-underwater problem. In some facets the two problems are quite similar, but in many there are significant differences. Concurrently with this research, Messere⁽³⁾ is attacking the underwater-to-underwater problem.

1.3 Outline of Attack

The problem will be attacked in three broad steps. First those quantities not found in the "above-water" problem are defined, examined, and illustrated when appropriate. Then the problem is formulated following the development in Chapter Two of Wrigley and Hovorka. Finally two general methods of solution of the problem are proposed, briefly analyzed and compared.

CHAPTER 11

QUANTITIES PECULIAR TO THE UNDERWATER FIRE CONTROL PROBLEM

2.1 Introduction

In beginning the investigation of the surface-to-underwater fire control problem, one is immediately struck with its points of difference with the "above-water" fire control problem. In the underwater problem, intelligence as to the target's position is received by sound waves which

- (1) travel slowly enough compared to target speeds that the above mentioned intelligence must be considered as past data;
- (2) travel in a medium where the speed of sound has enough variation within the volume of consideration that refractive effects cannot be ignored.

On the other hand, "above-water" electromagnetic radiation can be assumed to travel in straight lines for the purposes of the problem, and the intelligence of the target's position it conveys can be assumed to be current.

2.2 Splash Point

One way of considering the surface-to-underwater problem is to determine the position on the surface of the water, called the splash point, where a weapon should enter so that it will sink

vertically to the future position of the target, or in the case of homing weapons to the optimum position relative to the target to attack it. The geometrical features of the splash point are illustrated in figure 1. Using this approach the problem is that of a surface weapon station delivering a weapon to a given position on the surface of the water. The vector \bar{R}_s , splash range, is defined as the direction and distance from the present position of the weapon station to this given position (the splash point). In general, this vector is determined by predicting target motion.

2.3 The Water-Mass Coordinate Frame

The concept of target motion brings to mind the following question: target motion with respect to what coordinate frame? It is of course possible to generalize, but for the purposes of this thesis the water-mass frame is used.¹ This has been chosen for several reasons: the weapon station and the target move in it, the sound waves which are used to obtain target information travel in it, and it can be assumed that a weapon upon entering the water at the splash point will fall vertically in the water-mass, i.e., that any horizontal component of velocity with respect to the water-mass at time of water entry will be essentially brought to zero at once. The coordinate frame is arranged in the water-mass to yield horizontal and vertical components of vectors. These components are designated by a final subscript H or V as appropriate.

¹See the discussion of coordinate frames in Wrigley and Hovorka, pp. 5-7.

2.4 Transmission Time

In the "above-water" problem, intelligence as to the position of the target is usually assumed to be current. Such is not the case in the underwater problem. Transmission time, denoted by the symbol t_T , is defined as the interval of time required for sound to travel from the target to the weapon station sound detector. It is illustrated in figure 2 and quantitatively defined by the equation

$$t_T = \int_0^{R_a} \frac{dr}{v(r)} \quad (2.1)$$

where R_a is antecedent range: the distance from the present position of the sound detector to the position of the target t_T previously¹ and where $v(r)$ is the speed of sound as a function of the path it takes. In practice, of course, an average or standard value for the speed of sound is used, for example 1500 meters per second.⁽⁴⁾ For R_a equal to 3000 meters t_T is then equal to 2 seconds. In this time a 20 knot target will travel over 20 yards, a distance that cannot be neglected in the solution of the problem.

2.5 Line of Sight and Line of Position

The following quantities are defined in order to formulate the problem of determining target motion. Refer to figure 3.

\bar{l}_{LSO} - direction of the present line of sight: the reverse of the direction (as measured at the weapon station)

¹ It should be mentioned that R_a is a corrected quantity and not raw data. The actual range must be corrected for the refractive effects present.

of the sound reflected from the target t_T previously.

\bar{I}_{LPa} - direction of the antecedent line of position:

the direction of the vector from the present position of the weapon station (the sound detector) to the antecedent position of the target (measured t_T previously).

The preceding two quantities differ by what is called inaccuracy in the line of sight. This inaccuracy is a statistical quantity with a mean and a variance. Neither the mean nor the variance are known exactly, but they can be estimated in a statistical sense.

The mean of the inaccuracy is called error and the variations about it are uncertainty. Correction to the line of sight, symbolized (C)LS, is defined as the negative of the best estimate of error in the line of sight. It is determined by consideration of the speed of sound versus depth characteristics of the transmitting medium, assuming that the speed of sound at any one depth is constant over the water area involved (see assumption below).

Now

$$\overline{(C)LS} = (\bar{I}_{LS0} \times \bar{I}_{LPa}) \frac{(C)LS}{\sin (C)LS} \quad (2.2)$$

thus $\overline{(C)LS}$ is in the horizontal plane under the following two assumptions:

- (1) The effects of variation in salinity and pressure on the speed of sound are neglected.¹

¹Kinsler and Frey, p. 435.

(2) The gradient of water temperature is always vertical.

2.6 Target Velocity

Because of the inherent lag in target information caused by transmission time, present target velocity cannot be directly determined as in the "above-water" problem. Instead, antecedent target velocity, symbolized \bar{V}_{Ta} , is the available quantity used. It is defined as the direction and speed of motion of the target t_T prior to present time.

2.7 Sinking Time

Sinking time of the weapon, denoted t_s , is illustrated in figure 4. It is measured from the time of water entry to the time of expected detonation or time of commencing homing as appropriate. Sinking time will be an empirically determined quantity dependent upon the weapon and the depth to which it is expected to sink. This depth is the vertical component of the future line of position, which is defined in section 2.9.

2.8 Future Range

Figure 5 illustrates future range \bar{R}_F . It is the vector from the present position of the weapon station to the position of the target at future time $t_f + t_s$, where t_f is the time of flight of the weapon. \bar{R}_F is quantitatively defined by the following equation:

$$\bar{R}_F = R_a \bar{I}_{LPa} + \bar{V}_{Ta}(t_T + t_f + t_s) + \int_0^{t_T + t_f + t_s} \int_0^t \bar{V}_T(\tau) d\tau dt$$

(2.3)

where $\dot{\bar{V}}_T(\gamma)$ is target acceleration as a function of time. This acceleration cannot be predicted except in a statistical sense. Let the statistical "best guess" of the average value of $\dot{\bar{V}}_T(\gamma)$ over the time interval $t_T + t_f + t_s$ be symbolized $\dot{\bar{V}}_T^*$. Then equation (2-3) becomes

$$\bar{R}_F = R_a I_{LPa} + \bar{V}_{Ta}(t_T + t_f + t_s) + \frac{1}{2} \dot{\bar{V}}_T^*(t_T + t_f + t_s)^2 \quad (2-4)$$

2.9 Offset Range and Future Line of Position

Offset range, \bar{R}_{OFF} , is shown in figure 5. It is a vector used when homing weapons are employed and places the weapon at an optimum target angle and range with respect to the target at time $t_f + t_s$ after firing. The idea of offset range has to do with a "weighted" center of lethality. This concept, illustrated in figure 6, can be applied to any weapon that does not have to strike the target to detonate with lethal results. In the case of the proximity fuse the center of lethality is in fact the target itself since the velocities of the weapon fragments after burst are so much greater than the target's velocity that there is no measurable difference in the lethality of a burst equally distant ahead of or behind the target. Such is not the case with a homing torpedo. After arriving at the end of the offset range vector, it homes for the target using its own propulsion, which may or may not give it a speed advantage over the target. Clearly then the center of lethality for such a weapon is not at the target,

but generally ahead of the target. The exact position is determined by the characteristics of the weapon and \bar{V}_{Ta} . For non-homing weapons \bar{R}_{OFF} is, of course, zero.

The future line of position, symbolized \bar{LP}_F , is defined as the vector from the present position of the weapon station to the time of \bar{R}_{OFF} . As is indicated in figure 5:

$$\bar{LP}_F = \bar{R}_F + \bar{R}_{OFF} \quad (2-5)$$

2.10 Summary: The Determination of Splash Range

Finally it is seen from figure 5 that since the weapon must sink along \bar{LP}_{FV} to achieve its objective, the point of water entry must be at the tip of \bar{LP}_{FH} . Thus:

$$\bar{R}_s = \bar{LP}_{FH} \quad (2-6)$$

$$\bar{R}_s = \bar{R}_{FH} + \bar{R}_{OFFH} \quad (2-7)$$

CHAPTER III

FORMULATION OF THE PROBLEM

3.1 Introduction: Miss-Producing Effects

Chapter II considers some of the aspects of the surface-to-underwater fire control problem that differ from the "above-water" problem. Now the problem itself is formulated. As noted by Wrigley and Hovorka¹ there are three miss-producing effects:

- (1) Target motion
- (2) Curvature of the projectile's trajectory
- (3) Jump

In the problem of this thesis, target motion involves the travel of the target between its last known position (this position being that of the target t_f prior to firing) and its position at the time of expected detonation, or the time of commencing homing, as appropriate (this position being that of the target $t_f + t_s$ after firing). Unlike the "above-water" problem it also involves a displacement of the center of lethality from the target's position at the time of commencing homing. Since this displacement is dependent upon the target's motion (it would be zero if the target were stationary) it is included as a miss-producing effect involved

¹Wrigley and Hovorka, p. 24. This chapter follows their development closely.

with target motion. Figure 7 illustrates target motion as a miss-producing effect.

Trajectory curvature is made up, as in the "above-water" problem of the effects due to the forces that act on the projectile during its time of flight. It is illustrated in figure 8.

Similarly, jump is not altered by the special conditions of this thesis and represents the effect of factors that make the initial velocity of the projectile differ in direction from that of the weapon line, which is defined as the direction in which the weapon is aimed. Figure 9 illustrates it.

3.2 Corrections for Miss-Producing Effects

If the weapon line were to be oriented along the horizontal component of the antecedent line of position the three miss-producing effects mentioned above would all cause the projectile to miss the splash point. If a perfect set of corrections could be developed to apply to the weapon line prior to firing, the miss-producing effects would be completely nullified and the projectile would enter the water exactly at the splash point as desired. Toward this ideal the following corrections for miss-producing effects are developed:

- (1) Lead, which compensates for target motion effects.
- (2) Curvature correction, compensating for in-flight forces acting on the projectile.
- (3) Jump correction, to compensate for initial velocity effects.

These corrections are illustrated in figure 10.

3.3 Prediction Angle and the Prediction Angle Vector

Since each correction is a directional compensation it is therefore an angle. Hence the sum of these component angles is an angle and is defined as the prediction angle, measured from the horizontal component of the antecedent line of position to the weapon line. The vertical component of the antecedent line of position does not enter into the definition of prediction angle as the problem is formulated as a surface-to-surface problem with the projectile being fired to hit the splash point.

Under certain limitations the prediction angle P can be defined as a vector angle.¹ Consider the cross product of \bar{I}_{LPaH} with \bar{I}_{WL} :

$$\bar{I}_{LPaH} \times \bar{I}_{WL} = \bar{I}_{\perp(LP a H, WL)} \sin P \quad (3-1)$$

Now if P is a "small" angle, i.e., $\sin P = \tan P = P$ and $\cos P = 1$ within limits of allowable tolerances, the vector angle \bar{P} can be defined as

$$\bar{P} = \bar{I}_{\perp(LP a H, WL)} P \cong \bar{I}_{LPaH} \times \bar{I}_{WL} \quad (3-2)$$

Since the accuracies of measurable quantities involved in the problem of this thesis are not anywhere near those of the

¹Wrigley and Hovorka, p. 19.

"above-water" problem, the inaccuracies introduced by employment of the "small" angle assumption throughout this thesis will not materially effect the accuracy of the solution of the problem. Henceforth this "small" angle assumption will be valid, and will not produce any restrictions to the problem.

3.4 Lead

Lead is defined as the angle between the horizontal component of the antecedent line of position and the horizontal component of the future line of position. Unlike the "above-water" problem, the future line of position is the direction from the present position of the weapon station to the point below the splash point defined by the tip of the offset range vector. Thus the future line of position can be thought of as pointing toward a pseudo-target. Note that \bar{I}_{LPFH} is identical to \bar{R}_s/R_s . Figures 5 and 11 assist in understanding the following derivation:

Under the "small" angle assumption

$$\begin{aligned} \bar{L} &= \bar{I}_{LPaH} \times \bar{I}_{LPFH} \\ &= \frac{\bar{I}_{LPaH} \times \bar{R}_s}{R_s} \end{aligned} \quad (3-5)$$

Now

$$(1) \quad \bar{R}_s = \bar{R}_{FH} + \bar{R}_{OFFH} \quad (2-7)$$

$$(2) \quad R_s = V_{P(av)} t_f \quad (3-6)$$

where $V_{P(av)}$ is average projectile velocity

The horizontal component of eq. (2-4) gives

(3)

$$\bar{R}_{FH} = \bar{R}_{aH} + \bar{V}_{TaH}(t_T + t_f + t_s) + \frac{1}{2} \bar{V}_{TH}^* (t_T + t_f + t_s)^2 \quad (3-7)$$

$$\left[= \frac{\bar{I}_{LPaH} \times \bar{V}_{TaH}(t_T + t_f + t_s)}{V_{P(av)} t_f} + \frac{\bar{I}_{LPaH} \times \bar{V}_{TH}^* (t_T + t_f + t_s)^2}{2 V_{P(av)} t_f} + \frac{\bar{I}_{LPaH} \times \bar{R}_{OFFH}}{V_{P(av)} t_f} \right] \quad (3-8)$$

Now

$$(\bar{W}_{LPaH})_T = \frac{\bar{I}_{LPaH} \times \bar{V}_{TaH}}{R_{aH}} \quad (3-9)$$

where $(\bar{W}_{LPaH})_T$ is the angular velocity of the horizontal component of the antecedent line of position that is due to target motion.

$$\bar{W}_{LPaH} = (\bar{W}_{LPaH})_T + (\bar{W}_{LPaH})_{WS} \quad (3-10)$$

where \bar{W}_{LPaH} is the angular velocity of the horizontal component of the antecedent line of position and $(\bar{W}_{LPaH})_{WS}$ is the angular velocity of the horizontal component of the antecedent line of position that is due to weapon station motion.

Wrigley and Hovorka¹ have shown that

$$(\bar{W}_{LPaH})_{WS} = - \frac{\bar{I}_{LPaH} \times \bar{V}_{WS0}}{R_{aH}} \quad (3-11)$$

¹Wrigley and Hovorka, p. 32, figure 2-6.

where \bar{V}_{WSo} is weapon station velocity.

Thus, by combining and rearranging

$$\begin{aligned} \bar{C} = & \frac{R_{aH}}{V_{P(av)}} \frac{(t_T + t_f + t_s)}{t_f} \bar{W}_{LPaH} + \frac{\bar{I}_{LPaH} \times \bar{V}_{WSo}}{V_{P(av)}} \frac{(t_T + t_f + t_s)}{t_f} \\ & + \frac{\bar{I}_{LPaH} \times \bar{V}_{TH}^*}{2 V_{P(av)}} \frac{(t_T + t_f + t_s)^2}{t_f} + \frac{\bar{I}_{LPaH} \times \bar{R}_{OFFH}}{V_{P(av)} t_f} \end{aligned} \quad (3-12)$$

It must be noted that \bar{I}_{LPaH} cannot be measured, but \bar{I}_{LSoH} can. Fortunately, (C)LS is in the vertical plane under the assumptions made in the last chapter (see the section on line of sight and line of position) so \bar{I}_{LPaH} and \bar{I}_{LSoH} are identical. Similarly, while \bar{W}_{LPaH} cannot be measured, it is the same as \bar{W}_{LSoH} , the angular velocity of the horizontal component of the present line of sight, which can be instrumented.

3.5 Curvature Correction

Curvature correction is illustrated in figure 12 and is defined as a rotation from the horizontal component of the future line of position to the projectile line. Thus, under the "small" angle assumption the curvature correction vector is defined as follows:

$$\bar{C} = \bar{I}_{LPFH} \times \bar{I}_{PL} \quad (3-13)$$

where \bar{C} is the curvature correction

$\bar{I}_{PL} = \bar{V}_{PO}/V_{PO}$, the unit vector along the projectile line
 \bar{V}_{PO} is the projectile velocity at the time of firing

Splash range is given by

$$\bar{R}_s = \bar{V}_{PO} t_f + \int_0^{t_f} \int_0^t \bar{\dot{V}}_p(\tau) d\tau dt \quad (3-14)$$

where $\bar{\dot{V}}_p$ is the projectile acceleration

Splash range is also given by

$$\bar{R}_s = \bar{I}_{LPFH} R_s = \bar{I}_{LPFH} V_{p(av)} t_f \quad (3-15)$$

Substituting equations (3-14) and (3-15) into equation (3-13)

gives

$$\bar{C} = \frac{\left(\int_0^{t_f} \int_0^t \bar{\dot{V}}_p(\tau) d\tau dt \right) \times \bar{I}_{PL}}{V_{p(av)} t_f} \quad (3-16)$$

For the purposes of this section of the thesis the water-mass is assumed to be effectively inertial space and thus

$$\bar{\dot{V}}_p = \bar{f}_p \quad (3-17)$$

where \bar{f}_p is the sum of the principal specific forces (forces per unit mass) acting on the projectile during its flight.

These principal forces are:

- (1) Gravity, \bar{G} , the gravitational field intensity due to the mass attraction of the earth for the projectile.

- (2) Aerodynamic drag per unit mass; for Mach numbers encountered in the problem of this thesis, this is
 $-k_D V_{(AM)P} \bar{V}_{(AM)P}$, where k_D is an empirical coefficient and $\bar{V}_{(AM)P}$ is the projectile velocity in the air mass.
- (3) Lift per unit mass, $\bar{f}_{(li)}$.
- (4) Thrust per unit mass, $\bar{f}_{(th)}$, when the projectile is self-propelled.

Thus,

$$\bar{\dot{V}}_P = \bar{G} - k_D V_{(AM)P} \bar{V}_{(AM)P} + \bar{f}_{(li)} + \bar{f}_{(th)} \quad (3-18)$$

Integration of this equation involves line integrals, as the vectors are generally changing over the time interval of the integration. However, using average values of the vectors over the time interval:

$$\int_0^{t_f} \int_0^t \bar{\dot{V}}_P(\gamma) d\gamma dt = \frac{t_f^2}{2} \left[\bar{G} - k_{D(av)} V_{(AM)P(av)} \bar{V}_{(AM)P(av)} + \bar{f}_{(li)(av)} + \bar{f}_{(th)(av)} \right] \quad (3-19)$$

Substitution of equation (3-19) into equation (3-16) gives:

$$\bar{C} = \frac{t_f}{2 V_{P(av)}} \left[\bar{G} \times \bar{I}_{PL} - k_{D(av)} V_{(AM)P(av)} \bar{V}_{(AM)P(av)} \times \bar{I}_{PL} + \bar{f}_{(li)(av)} \times \bar{I}_{PL} + \bar{f}_{(th)(av)} \times \bar{I}_{PL} \right] \quad (3-20)$$

It should be noted that no drift term is present since ASW projectiles have no significant spin.

3.6 Jump Correction

Figure 13 illustrates jump correction, which is the angular correction needed to compensate for the non-parallelism of the weapon line and the initial projectile velocity. It is measured from the projectile line to the weapon line. The jump correction vector is the negative of the jump vector, \bar{J} , and under the "small" angle assumption is defined below:

$$-\bar{J} \equiv \bar{I}_{PL} \times \bar{I}_{WL} \quad (3-21)$$

For the problem of this thesis, $-\bar{J}$ is made up entirely of weapon station velocity jump correction. It is required because a projectile leaving the weapon station with a velocity $\bar{V}_{[(WS)P]O}$ relative to the weapon station has the total velocity:

$$\bar{V}_{Po} = \bar{V}_{[(WS)P]O} + \bar{V}_{WSO} \quad (3-22)$$

where \bar{V}_{WSO} is the weapon station velocity at the time of firing.

Windage jump¹ is not present as ASW weapons have no significant spin.

Since $\bar{I}_{PL} = \bar{V}_{Po}/V_{Po}$ and $\bar{V}_{[(WS)P]O}$ is along \bar{I}_{WL}

$$-\bar{J} = \frac{\bar{V}_{WSO} \times \bar{I}_{WL}}{V_{Po}} \quad (3-23)$$

3.7 Summary

Prediction angle, \bar{P} , is defined as a vector rotation from the horizontal component of the antecedent line of position to

¹Wrigley and Hovorka, p. 39.

the weapon line. Under the "small" angle assumption the following equation is valid:

$$\bar{P} = \bar{I}_{LPaH} \times \bar{I}_{WL} \quad (3-2)$$

Thus, prediction is given in terms of lead, curvature correction, and jump correction as:

$$\bar{P} = \bar{L} + \bar{C} - \bar{J} \quad (3-24)$$

Upon substitution of the previously derived equations (3-12), (3-20), and (3-23), prediction angle is seen to be made up of the following terms:

$$\begin{aligned} \bar{P} = & \left\{ \frac{R_{aH}}{V_{P(av)}} \frac{(t_T + t_f + t_s)}{t_f} \bar{W}_{LPaH} + \frac{\bar{I}_{LPaH} \times \bar{V}_{Wso} (t_T + t_f + t_s)}{V_{P(av)} t_f} \right\} \\ & \left. \begin{array}{cc} \text{Horizontal component of line of} & \text{Weapon station} \\ \text{position angular velocity} & \text{velocity} \end{array} \right\} \text{Lead} \\ & + \left\{ \frac{\bar{I}_{LPaH} \times \bar{V}_{TH}^* (t_T + t_f + t_s)^2}{2 V_{P(av)} t_f} + \frac{\bar{I}_{LPaH} \times \bar{R}_{OFFH}}{V_{P(av)} t_f} \right\} \\ & \left. \begin{array}{cc} \text{Horizontal target acceleration} & \text{Horizontal offset} \end{array} \right\} \\ & + \frac{t_f}{2 V_{P(av)}} \left\{ \bar{G} \times \bar{I}_{PL} - k_{D(av)} V_{(AM)P(av)} \bar{V}_{(AM)P(av)} \times \bar{I}_{PL} \right. \\ & \left. + \left(\bar{F}_{(li)(av)} + \bar{F}_{(th)(av)} \right) \times \bar{I}_{PL} \right\} + \\ & \left. \begin{array}{cc} \text{Gravity drop} & \text{Aerodynamic drag} \\ \text{Lift and thrust} & \end{array} \right\} \text{Curvature Correction} \end{aligned}$$

$$+ \frac{\overline{V_{wsa}} \times \overline{I_{WL}}}{V_{Po}} \quad \left. \vphantom{\frac{\overline{V_{wsa}} \times \overline{I_{WL}}}{V_{Po}}} \right\} \begin{array}{l} \text{Jump} \\ \text{Correction} \end{array} \quad (3-25)$$

Velocity jump

The entire development is summarized in derivation summary 3-1.

DERIVATION SUMMARY 3-1

$$\bar{P} = \bar{L} + \bar{C} - \bar{J} \quad (3-24)$$

By definition:

$$\bar{L} \equiv \bar{I}_{LPaH} \times \bar{I}_{LPFH} \quad (3-5)$$

But $\bar{I}_{LPFH} \equiv \bar{R}_S / R_S$

and $\bar{R}_S = \bar{R}_{FH} + \bar{R}_{OFFH} \quad (2-7)$

$$\begin{aligned} \bar{R}_F &= \bar{R}_a + \bar{V}_{Ta} (t_T + t_f + t_s) \\ &\quad + \frac{1}{2} \bar{V}_T^* (t_T + t_f + t_s)^2 \end{aligned} \quad (2-4)$$

Taking the horizontal component of \bar{R}_F

$$\bar{R}_{FH} = \bar{R}_{aH} + \bar{V}_{TaH} (t_T + t_f + t_s) + \frac{1}{2} \bar{V}_{TH}^* (t_T + t_f + t_s)^2 \quad (3-7)$$

For the projectile to hit the splash point

$$R_S = V_{p(av)} t_f \quad (3-6)$$

So by combining and substituting

$$\begin{aligned} \bar{L} &= \frac{\bar{I}_{LPaH} \times \bar{V}_{TaH} (t_T + t_f + t_s)}{V_{p(av)} t_f} + \frac{\bar{I}_{LPaH} \times \bar{V}_{TH}^* (t_T + t_f + t_s)^2}{2 V_{p(av)} t_f} + \frac{\bar{I}_{LPaH} \times \bar{R}_{OFFH}}{V_{p(av)} t_f} \end{aligned} \quad (3-8)$$

Now

$$(\bar{W}_{LPaH})_T = \frac{\bar{I}_{LPaH} \times \bar{V}_{TaH}}{R_{aH}} \quad (3-9)$$

$$\bar{W}_{LPaH} = (\bar{W}_{LPaH})_T + (\bar{W}_{LPaH})_{WS} \quad (3-10)$$

$$(\bar{W}_{LPaH})_{WS} = - \frac{\bar{I}_{LPaH} \times \bar{V}_{WSo}}{R_{aH}} \quad (3-11)$$

So

$$\begin{aligned} \bar{C} = & \frac{R_{aH} (t_T + t_f + t_s)}{V_{P(av)} t_f} \bar{W}_{LPaH} + \frac{\bar{I}_{LPaH} \times \bar{V}_{WSo} (t_T + t_f + t_s)}{V_{P(av)} t_f} \\ & + \frac{\bar{I}_{LPaH} \times \bar{V}_{TH}^* (t_T + t_f + t_s)^2}{2 V_{P(av)} t_f} + \frac{\bar{I}_{LPaH} \times R_{OFFH}}{V_{P(av)} t_f} \end{aligned} \quad (3-12)$$

By definition:

$$\bar{C} \equiv \bar{I}_{LPFH} \times \bar{I}_{PL} \quad (3-13)$$

But $\bar{I}_{PL} \equiv \bar{V}_{po} / V_{po}$

Now

$$\bar{R}_S = \bar{V}_{Po} t_f + \int_0^{t_f} \int_0^t \bar{V}_P(\tau) d\tau dt \quad (3-14)$$

Also

$$\begin{aligned} \bar{R}_S &= \bar{I}_{LPFH} R_S \\ &= \bar{I}_{LPFH} V_{P(av)} t_f \end{aligned} \quad (3-15)$$

Thus

$$\bar{C} = \frac{\left(\int_0^{t_f} \int_0^t \bar{\dot{V}}_p(\tau) d\tau dt \right) \times \bar{I}_{PL}}{V_{P(av)} t_f} \quad (3-16)$$

Now

$$\bar{\dot{V}}_p = \bar{f}_p \quad (3-17)$$

$$\bar{\dot{V}}_p = \bar{G} - k_D V_{(AM)P} \bar{V}_{(AM)P} + \bar{f}_{(li)} + \bar{f}_{(th)} \quad (3-18)$$

Using average values

$$\int_0^{t_f} \int_0^t \bar{\dot{V}}_p(\tau) d\tau dt = \frac{t_f^2}{2} \left[\bar{G} - k_{D(av)} V_{(AM)P(av)} \bar{V}_{(AM)P(av)} + \bar{f}_{(li)(av)} + \bar{f}_{(th)(av)} \right] \quad (3-19)$$

So

$$\bar{C} = \frac{t_f}{2 V_{P(av)}} \left[\bar{G} \times \bar{I}_{PL} - k_{D(av)} V_{(AM)P(av)} \bar{V}_{(AM)P(av)} \times \bar{I}_{PL} + \bar{f}_{(li)(av)} \times \bar{I}_{PL} + \bar{f}_{(th)(av)} \times \bar{I}_{PL} \right] \quad (3-20)$$

By definition:

$$- \bar{J} \equiv \bar{I}_{PL} \times \bar{I}_{WL} \quad (3-21)$$

But $\bar{I}_{PL} \equiv \bar{V}_{po} / V_{po}$

Now $\bar{V}_{po} = \bar{V}_{[(WS)P]o} + \bar{V}_{WSo}$ (3-22)

But $\bar{V}_{[(WS)P]o} = V_{[(WS)P]o} \bar{I}_{WL}$

So

$$- \bar{J} = \frac{\bar{V}_{WSo} \times \bar{I}_{WL}}{V_{po}} \quad (3-23)$$

Finally, from equations (3-24), (3-12), (3-20) and (3-23)

$$\begin{aligned} \bar{P} = & \frac{R_{aH}}{V_{P(av)}} \frac{(t_T + t_f + t_s)}{t_f} \bar{W}_{LPaH} + \frac{\bar{I}_{LPaH} \times \bar{V}_{WSo} (t_T + t_f + t_s)}{V_{P(av)} t_f} \\ & + \frac{\bar{I}_{LPaH} \times \bar{V}_{TH}^* (t_T + t_f + t_s)^2}{Z V_{P(av)} t_f} + \frac{\bar{I}_{LPaH} \times \bar{R}_{OFFH}}{V_{P(av)} t_f} \\ & + \frac{t_f}{Z V_{P(av)}} \left[\bar{G} \times \bar{I}_{PL} - K_{D(av)} V_{(AM)P(av)} \bar{V}_{(AM)P(av)} \times \bar{I}_{PL} \right. \\ & \quad \left. + (\bar{F}_{(ii)(av)} + \bar{F}_{(th)(av)}) \times \bar{I}_{PL} \right] \\ & + \frac{\bar{V}_{WSo} \times \bar{I}_{WL}}{V_{Po}} \end{aligned}$$

CHAPTER IV

SOLUTION OF THE PROBLEM

4.1 Introduction

The preceeding two chapters have defined certain quantities, given a kinematic and geometric look at the problem, formulated the problem, and finally derived an expression for prediction angle. If all the quantities involved in this expression could be measured or computed (or even statistically "best-guessed" at) the problem would be solved. The solution, then, revolves around these quantities.

Many of the quantities involved are obtained in the same manner as in the "above-water" fire control problem. However, attention will be focused on those quantities that are peculiar to the underwater problem. All of the peculiarities occur in the lead part of the prediction angle and come about primarily as a result of using relatively slowly traveling sound waves to determine the position of the target. In addition, the quantity t_s is present as a consequence of the target's being below the surface of the water.

4.2 Information Rate

The use of sound causes an appreciable transmission time, as discussed in chapter II, a typical value being two seconds.

Furthermore the relatively low velocity of sound, about 1500 meters per second, means that sound pulses must be sent out at well separated intervals of time rather than semi-continuously as in radar. For example in radar 800 pulses per second is a typical rate⁽⁵⁾ giving a maximum unambiguous range of slightly less than 200 kilometers, while for a maximum unambiguous range of 7500 meters using sound waves in water the interval between pulses must be ten seconds. Under the conditions of the example the best information rate possible for the underwater target is one piece of information every ten seconds. Figure 14 illustrates the concept of this section.

4.3 Transformation of Target Information

Another complication comes about from the fact that it is not practical to stabilize the sound transducer against the angular motion of the weapon station. This means that information as to the location of the target is available only referred to the structure of the weapon station. A coordinate transformation must be used to transform target information into a frame that can be instrumented and related to the water-mass frame, in which the computation of the prediction angle is to be carried out. An example of this process is described in Appendix A.

4.4 The Triangulation Method

If successive positions of the target are used to determine lead, the following expression can be used:

$$\begin{aligned} \left[= \frac{\bar{I}_{LPaH} \times \bar{V}_{TaH} (t_T + t_f + t_s)}{V_{P(av)} t_f} + \frac{\bar{I}_{LPaH} \times \bar{R}_{OFFH}}{V_{P(av)} t_f} \right. \\ \left. + \frac{\bar{I}_{LPaH} \times \bar{V}_{TH}^* (t_T + t_f + t_s)^2}{2 V_{P(av)} t_f} \right] \end{aligned}$$

Horizontal target motion Horizontal offset

Horizontal Target Acceleration

(3-8)

The quantity \bar{V}_{TaH} is obtained by coordinatizing target positions in the water-mass frame (see fig. 15). By subtracting successive target positions its change in position relative to the weapon station $\Delta \bar{R}_{(WS)T}$ can be calculated. Since the weapon station velocity and the time between target positions are known, the change in weapon station position, $\Delta \bar{R}_{WS}$, can be calculated and combined with the previously computed change in target position relative to the weapon station. This gives the change in target position in the water-mass $\Delta \bar{R}_T$. The horizontal component of this change divided by the time between target positions, Δt , is \bar{V}_{TaH} and the vertical component of the change divided by the same time interval is \bar{V}_{TaV} . Thus, \bar{V}_{Ta} is computed. This quantity, together with the type of weapon used, determines \bar{R}_{OFF} and hence \bar{R}_{OFFH} . \bar{V}_T^* is not directly available from target information. It might be computed by dividing the change between successive values of \bar{V}_{Ta} by the time interval between them and assuming a constant acceleration over this interval. It also could be set in to the computer by hand. Transmission time, t_T , is empirically determined. The quantity \bar{I}_{LPaH} is, of course, available as \bar{I}_{LSOH} ,

and all the other quantities in equation (3-8) are determined as in the "above-water" problem. Thus, lead can be computed. Curvature correction and jump correction deal with "above-water" effects and are computed as in the "above-water" problem. The method of solution of this section is called the triangulation method in this thesis.

4.5 The Controlled Line Method

In this section the original expression for lead, equation (3-12), is used. The quantity \bar{W}_{LSO} must be measured in order to get \bar{W}_{LPaH} . As noted by Wrigley and Hovorka¹, the line on the fire control equipment that tracks the line of sight is called the tracking line, or indicated line of sight, and angular velocity of this line is the best information available as to the quantity \bar{W}_{LSO} . Since it is not feasible to stabilize the sound transducer, the method of this section could use either of two approaches:

- (1) Use a stabilized dummy tracking line and an unstabilized tracking line.
- (2) Transform the target information prior to displaying it.

Using the first approach, the components of dummy tracking line orientation, expressed in the reference coordinate system of Appendix A, would be transformed by the inverse of the matrix of equation (A-8) into components in the weapon station structure. These components would position a tracking line on displays of unstabilized target information. A lack of coincidence² between

¹Wrigley and Hovorka, p. 53

²Here coincidence is used in the sense of servo null: reducing the difference to the smallest value commensurate with the servo configuration, not necessarily to zero.

this tracking line and the displayed line of sight would give rise to a tracking inaccuracy. Thus, a tracking inaccuracy correction would have to be generated. This correction is denoted $(C)TL$ and is called correction to the tracking line. Illustrated in figure 16, it is the angle from the tracking line to the line of sight. In the process of solving the problem it would be nulled¹ and thus would be a "small" angle. The vector representation of this angle, $(C)\overline{TL}$, would be coordinatized in the weapon station structure. As shall be seen shortly, it would have to be transformed into water-mass coordinates using the matrix of equation (4-8) before it would be useful in solving the problem.

Using the second approach, the target data would be transformed into water-mass coordinates prior to display. The display equipment, although physically a part of the weapon station structure, would model the water-mass frame. The orientation of the dummy tracking line would directly position the tracking line of the displays and $(C)\overline{TL}$ would be coordinatized in the water-mass frame.

Since the water-mass frame can be related to inertial space, an attractive means of stabilizing the dummy tracking line is presented by the space integrator. This device is discussed in detail by Draper, Wrigley, and Grohe⁽⁶⁾. In essence, the space integrator performs two functions: (1) With no command input it holds the direction of a controlled line constant in inertial space in the

¹Here coincidence is used in the sense of a servo null: reducing the difference to the smallest value commensurate with the servo configuration, not necessarily to zero.

face of interferences; (2) With an input command it gives the controlled line an angular velocity with respect to inertial space that is proportional to the input. So if some input to this device can be found that will enable its controlled line to track the line of sight, the controlled line will be the dummy tracking line and the input command to the device will be proportional to the angular velocity with respect to inertial space of the line of sight. The horizontal component of this quantity is then the desired quantity \bar{W}_{LSoH} . There are two questions to be answered: (1) Can the water-mass frame be considered effectively inertial? It can, as the small errors introduced by this assumption are insignificant compared with uncertainties in the line of sight, for example: The line of sight is assumed for the sake of generality, to have an uncertainty of 10 milliradians, which is a realistic figure. The interval between successive bits of target information is 10 seconds. Then the uncertainty in W_{LSo} is 2 mr/sec. Assuming that the rotation of the water-mass with respect to the earth is of lesser magnitude than earth rate, i.e., the problem is not being worked near a whirlpool, then the difference between angular velocity in the water-mass and inertial angular velocity is no greater than earth rate, which is 0.0729 mr/sec. As this difference is much less than 2 mr/sec, the assertion is correct. The second question to be answered is: (2) What is a suitable command input to the space integrator? Since the space integrator operates with respect to inertial space, the input to it must be expressed in inertial space. Correction to the tracking line,

expressed in the water-mass frame, which has been shown to be effectively inertial, is a suitable input when properly modified. It will drive the controlled line so that for a constant \bar{W}_{LSO} , the tracking line will be coincident with the line of sight each time the line of sight is displayed. As an example, modify the signal proportional to $(C)\overline{TL}$ by multiplying it by R_a^2 and passing the product through a parallel integrator and bypass. Add the output of the parallel elements, divide by R_a^2 , and use the resulting signal as the input command to the space integrator (see figure 17). If the system starts with an initial $(C)\overline{TL}$, the integrator will build up a charge while $(C)\overline{TL}$ is being nulled. For a constant \bar{V}_{Ta} this integrator charge will give the correct signal to drive the space integrator at \bar{W}_{TL} equal to \bar{W}_{LSO} with $(C)\overline{TL}$ nulled.

The favorable answers to the two questions above indicate that the problem can be instrumented in this manner. With \bar{W}_{LPAH} obtainable from \bar{W}_{LSO} , the quantities t_T , t_s , \bar{T}_{LPAH} , and \bar{V}_T^* would enter the problem solution as in section 4.4. With the exception of \bar{R}_{OFFH} all other quantities in equation (3-25) would be determined as in the "above-water" problem. However, to get \bar{R}_{OFFH} , \bar{V}_{Ta} must be known. It would be determined essentially as in section 4.4. This indirect requirement for \bar{V}_{Ta} is a disadvantage of this method.

In "above-water" systems the instrumentation of the tracking line as the controlled line of a space integrator is common. Electromagnetic radiation is used and $(C)\overline{TL}$ can be considered as always available. This is not so in the underwater problem.

(c) \overline{TL} is available only each time line of sight information appears on the displays. This occurs only when a sound pulse is received. Thus, this method of solving the problem involves sampled data. The charge on the integrator discussed earlier in this section acts as a memory and drives the space integrator between bits of data, but a measure of the coincidence of the tracking line with the line of sight is available only with the receipt of a sound pulse from the target.

The method of solution employing the instrumentation described in this section is called the controlled line method in this thesis.

4.6 A Simple Analysis of the Preceding Two Methods

How well do the preceding two methods of solution do the job of instrumenting the perfect set of corrections mentioned in section 3.2? This analysis will compare the propagation of uncertainties in target position through the two methods, since the methods differ only in their computation of lead. Specifically, the following two expressions that give target motion (less acceleration) must be compared:

(1) From eq. (3-8)

$$\frac{\overline{I}_{LPaH} \times \overline{V}_{TaH}}{V_{P(av)}} \frac{(t_T + t_f + t_s)}{t_f}$$

(2) From eq. (3-12)

$$\frac{R_{aH}}{V_{P(av)}} \frac{(t_T + t_f + t_s)}{t_f} \bar{W}_{LPaH} + \frac{\bar{I}_{LPaH} \times \bar{V}_{WSo}}{V_{P(av)}} \frac{(t_T + t_f + t_s)}{t_f}$$

The other terms in equation (3-8) also appear in exactly the same form in equation (3-12). Further, since $\frac{t_T + t_f + t_s}{V_{P(av)} t_f}$ is common to both expressions, the comparison is reduced to that between $\bar{I}_{LPaH} \times \bar{V}_{TaH}$ and $R_{aH} \bar{W}_{LPaH} + \bar{I}_{LPaH} \times \bar{V}_{WSo}$.

$$\text{Now } \bar{W}_{LPaH} = (\bar{W}_{LPaH})_T + (\bar{W}_{LPaH})_{WS} \quad (3-10)$$

$$(\bar{W}_{LPaH})_{WS} = - \frac{\bar{I}_{LPaH} \times \bar{V}_{WSo}}{R_{aH}} \quad (3-11)$$

$$\text{So } R_{aH} \bar{W}_{LPaH} + \bar{I}_{LPaH} \times \bar{V}_{WSo} = R_{aH} (\bar{W}_{LPaH})_T \quad (4-1)$$

But

$$(\bar{W}_{LPaH})_T = \frac{\bar{I}_{LPaH} \times \bar{V}_{TaH}}{R_{aH}} \quad (3-9)$$

$$\text{So } R_{aH} (\bar{W}_{LPaH})_T = \bar{I}_{LPaH} \times \bar{V}_{TaH} \quad (4-2)$$

Finally, from equations (4-1) and (4-2)

$$\bar{I}_{LPaH} \times \bar{V}_{TaH} = R_{aH} \bar{W}_{LPaH} + \bar{I}_{LPaH} \times \bar{V}_{WSo} \quad (4-3)$$

In the controlled line method, \bar{W}_{LPaH} is dependent upon input bits of information, not a continuous flow as in "above-water" systems.

However, if \bar{V}_{Ta} is assumed constant, the signal modification scheme outlined in the preceding section contains a constant quantity: $k R_a^2 \bar{W}_{LSO}$ where k is a constant of proportionality.

This was first observed by Kenneth Wallace about ten years ago.

Since the quantity R_a can be generated by the "memory" of the

computer between input bits of information, \bar{W}_{LSo} can be kept up to date and the \bar{W}_{LPaH} determined by the controlled line method will correspond to the latest antecedent line of position. Thus, equation (4-3) is valid for a comparison of the two methods, and indeed shows them to be effectively the same. Thus, the uncertainty in lead caused by uncertainty in target information will be the same for both methods. A quantitative measure of this uncertainty is given by the following illustrative example:

Assume a non-homing weapon is used and target acceleration is zero.

Let $R_a = 2000$ yards and $R_{aH} = 1992$ yards

Then $t_T = 1$ second as the speed of sound is assumed here as 2000 yards per second.

Let $V_{p(av)} = 1600$ feet per second

$t_f = 4$ seconds

$t_s = 5$ seconds

Let uncertainty in the horizontal component of the line of sight, $(U)\overline{LS}_{oH} = 5$ milliradians.

Let maximum unambiguous range be 5000 yards, giving an information rate of 1/5 bit per second.

Then $(U)\bar{W}_{LSoH} = 2 \text{ mr/sec} = (U)\bar{W}_{LPaH}$

Let $(U)R_{aH} = 20$ yards

$(U)V_{WSo} \overline{LPaH} = 1 \text{ foot/sec}$

$V_{WSo} \overline{LPaH} = 30 \text{ feet/sec}$

$W_{LPaH} = 10 \text{ mr/sec}$

Now under the assumptions

$$\bar{C} = \frac{R_{aH}}{V_{P(av)}} \frac{(t_T + t_f + t_s)}{t_f} \bar{W}_{LPaH} + \frac{\bar{I}_{LPaH} \times \bar{V}_{WS0}}{V_{P(av)}} \frac{(t_T + t_f + t_s)}{t_f}$$

(4-4)

$$\bar{C} = \left[\frac{3(1992 \pm 20)}{1600} \frac{10}{4} (10 \pm 2) \times 10^{-3} + \frac{(30 \pm 1) \times 10}{1600 \times 4} \right] \bar{I}_v$$

$$\bar{C} = \frac{10}{6400} [(5.976 \pm .060)(10 \pm 2) + (30 \pm 1)] \bar{I}_v$$

Since $\frac{(U)\bar{W}_{LPaH}}{\bar{W}_{LPaH}}$ is not $\ll 1$, conventional methods of error analysis are not applicable and a straightforward computation is used.

$$\bar{C}_{MAX} = \frac{10}{6400} [6.036 \times 12 + 31] \bar{I}_v$$

$$\bar{C}_{MAX} = .162 \bar{I}_v$$

$$\bar{C}_{MIN} = \frac{10}{6400} [5.916 \times 8 + 29] \bar{I}_v$$

$$\bar{L}_{MIN} = .119 \bar{I}_V$$

Defining lead uncertainty, $(U)\bar{L}$, as follows:

$$(U)\bar{L} = \frac{1}{2} (\bar{L}_{max} - \bar{L}_{min}) \quad (4-5)$$

$$(U)\bar{L} = \frac{1}{2} (.162 - .119) \bar{I}_V = .022 \bar{I}_V \quad (4-6)$$

Both methods are classified as TT systems under the scheme of Wrigley and Hovorka¹. Although it would be possible to configure them otherwise, there is no reason for so doing. Indeed, Markey⁽⁷⁾ has concluded that the three dimensional TT system is, in general, better than a WW system, assuming independent operation of axes.

4.6 Summary

This chapter considers the solution of the problem. The sampled data nature of target information is pointed out, as is the required transformation of this information. Two methods for solving the problem, the triangulation method and the controlled line method, are described and the methods analyzed. This analysis finds them to be effectively the same. Equation (4-3) relates the quantities that differ in the two methods.

It would seem then, that there is little to choose between the two methods with regard to accuracy considerations. The

¹Wrigley and Hovorka, p. 57.

controlled line method does have the disadvantage of requiring an additional computation of \bar{V}_{Ta} , needed to determine \bar{R}_{OFF} when homing weapons are used.

An illustrative example of the propagation of uncertainties yields an uncertainty in lead of 22 milliradians under the assumed conditions.

CHAPTER V
SUMMARY AND CONCLUSIONS

5.1 Problems Caused by the Target's Being Underwater

The use of sound to obtain target information is the big difference between the "above-water" and the surface-to-underwater fire control problem. This thesis has shown in the example of section 2.4 that a finite transmission time of sound from the target to the weapon station requires the use of past data to solve the problem. Concomitant with this is the concept of a slow information rate, leading to having some data available only as sampled data with a sampling rate which cannot be increased beyond a fixed limit set by unambiguous range considerations.

The fact that water temperature variations commonly encountered at sea cause the speed of sound in water to vary significantly requires corrections for refractive effects. The footnote on page 5 and section 2.5 mention two of these corrections. Fortunately, the angular correction to the line of sight lies essentially in the vertical plane, a fact which is of assistance in the instrumentation of the problem.

Although not associated with the use of sound, the concept of an offset center of lethality, caused by the fact that the

speeds of homing weapons are of the same order as target speeds, is used in formulating the problem of this thesis. This concept leads to the development of an offset range vector (section 2.9).

Finally, sinking time, t_s , not found in the "above-water" problem, was used to account for the interval of time from water entry of the weapon at the splash point to the arrival of the weapon at the point of detonation or the optimum attack position as appropriate.

5.2 Methods for Solving the Surface-to-Underwater Fire Control Problem

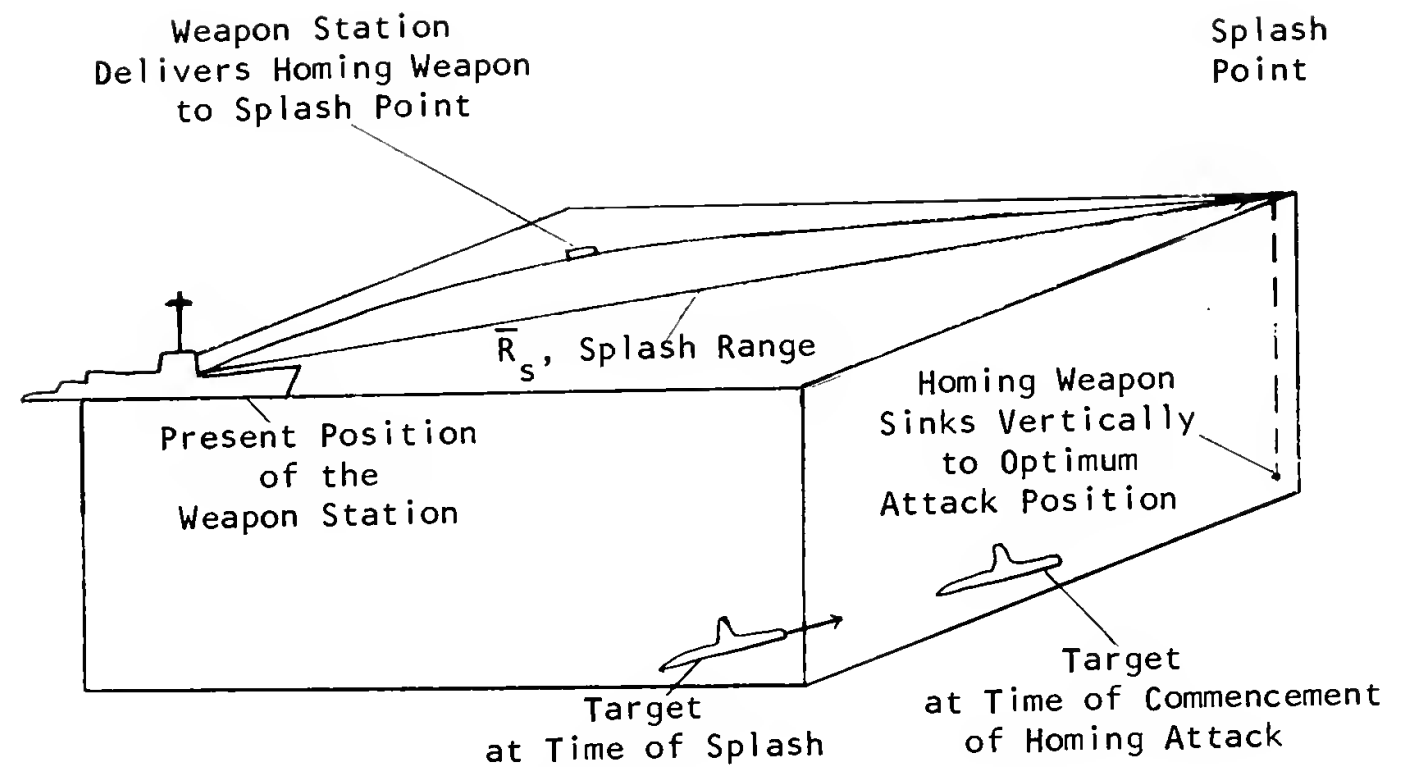
Two methods for solving the problem are discussed in this thesis: the triangulation method and the controlled line method. A brief analysis indicates that both methods compute prediction angle in essentially the same manner, using the same inputs to develop essentially the same quantities by slightly different means. Thus, the two methods are shown to be effectively the same (equation 4-3) so that inaccuracies in input information propagate in the same manner in both methods, leaving no choice between them on that account. In section 4.6 it is noted that the controlled line method has the disadvantage of an additional required computation for \bar{V}_{Ta} when homing weapons are used.

5.3 Suggestions for Further Work

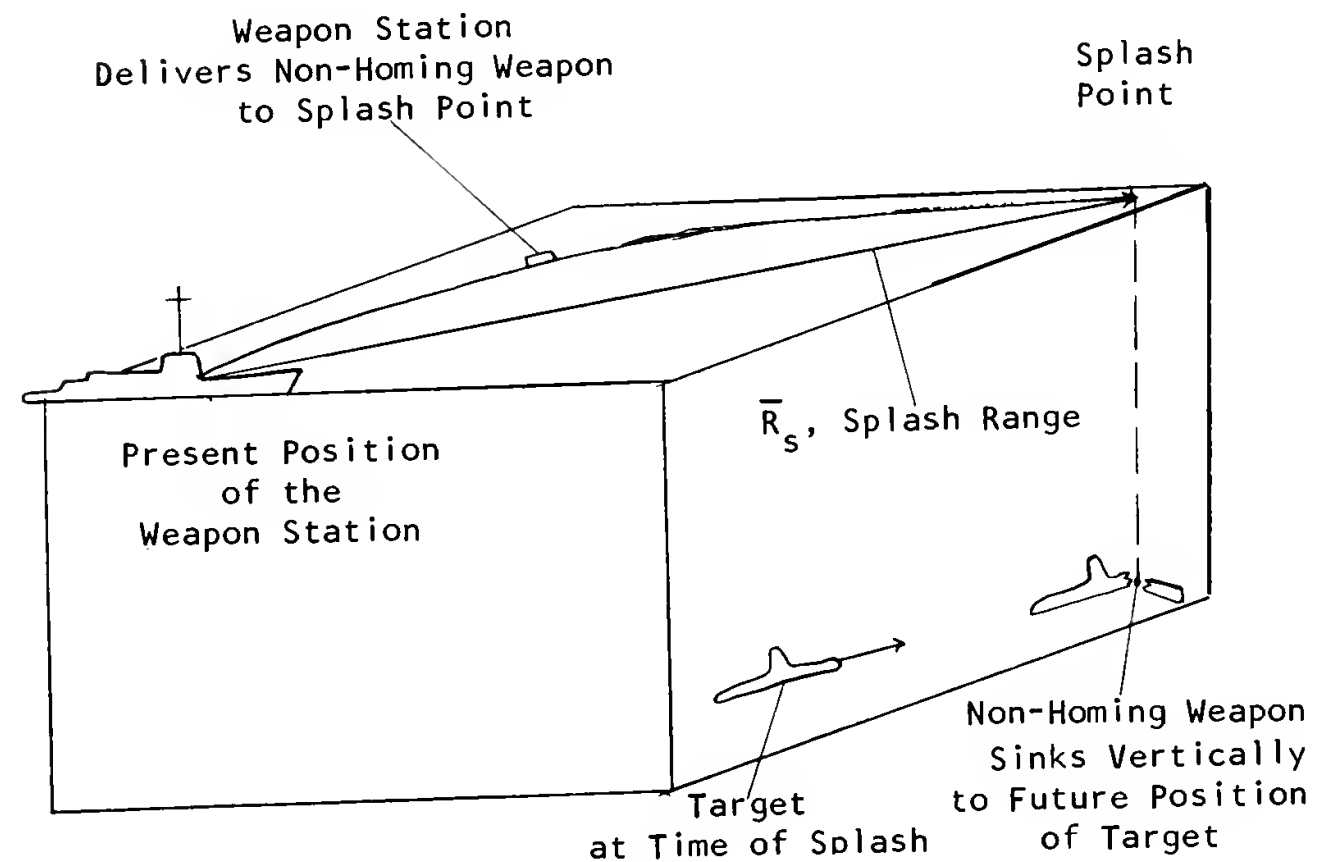
Since this thesis is an initial attack on the surface-to-underwater fire control problem from the viewpoint expressed by Wrigley and Hovorka, more work remains to be done. An

investigation of the sampled data aspects of the problem is one area.

A frequency diversity scheme might be used to increase the information rate. This would involve "hardware" modifications. The feasibility of the idea might be investigated.



a) The Homing Case



b) The Non-Homing Case

Figure 1. Geometrical Features of the Splash Point

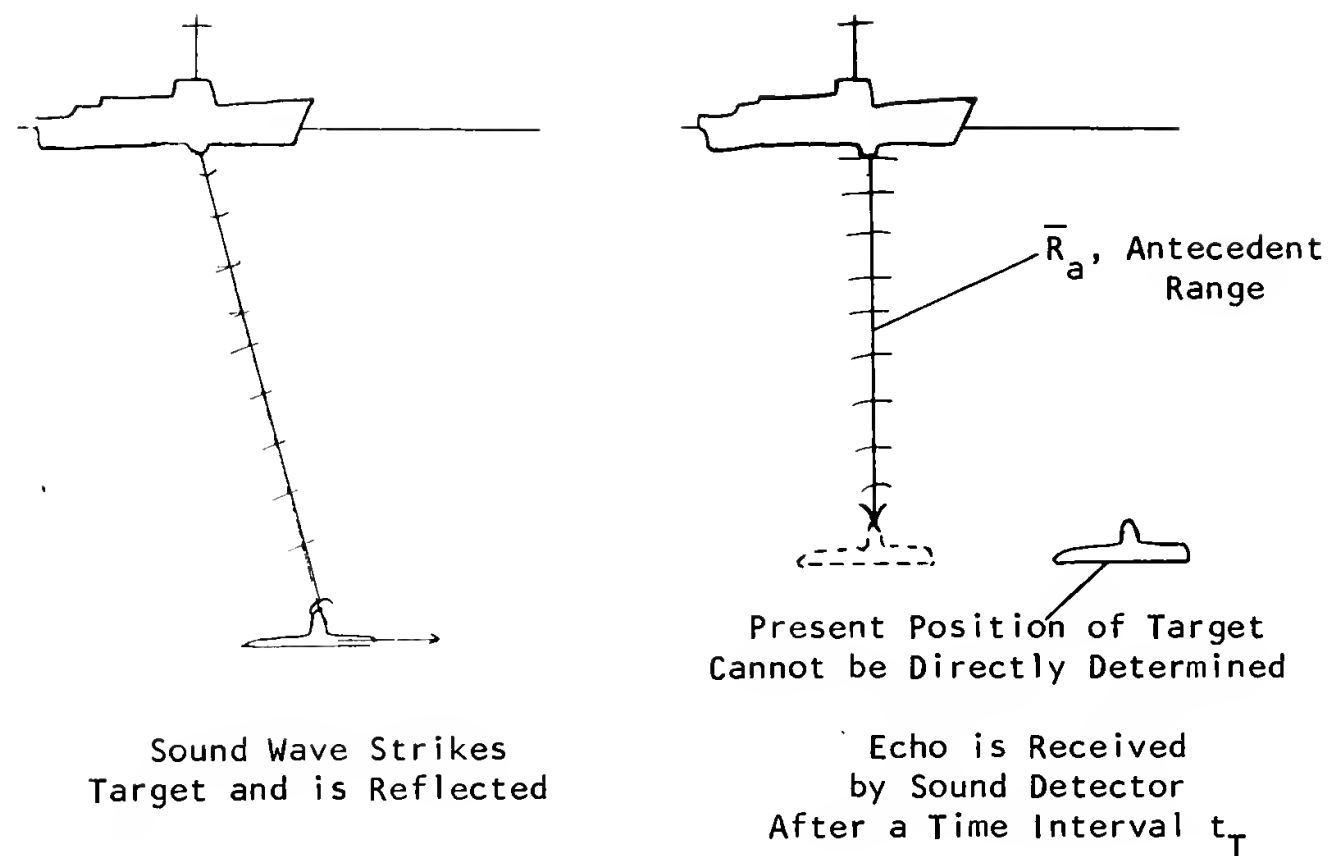


Figure 2. Transmission Time

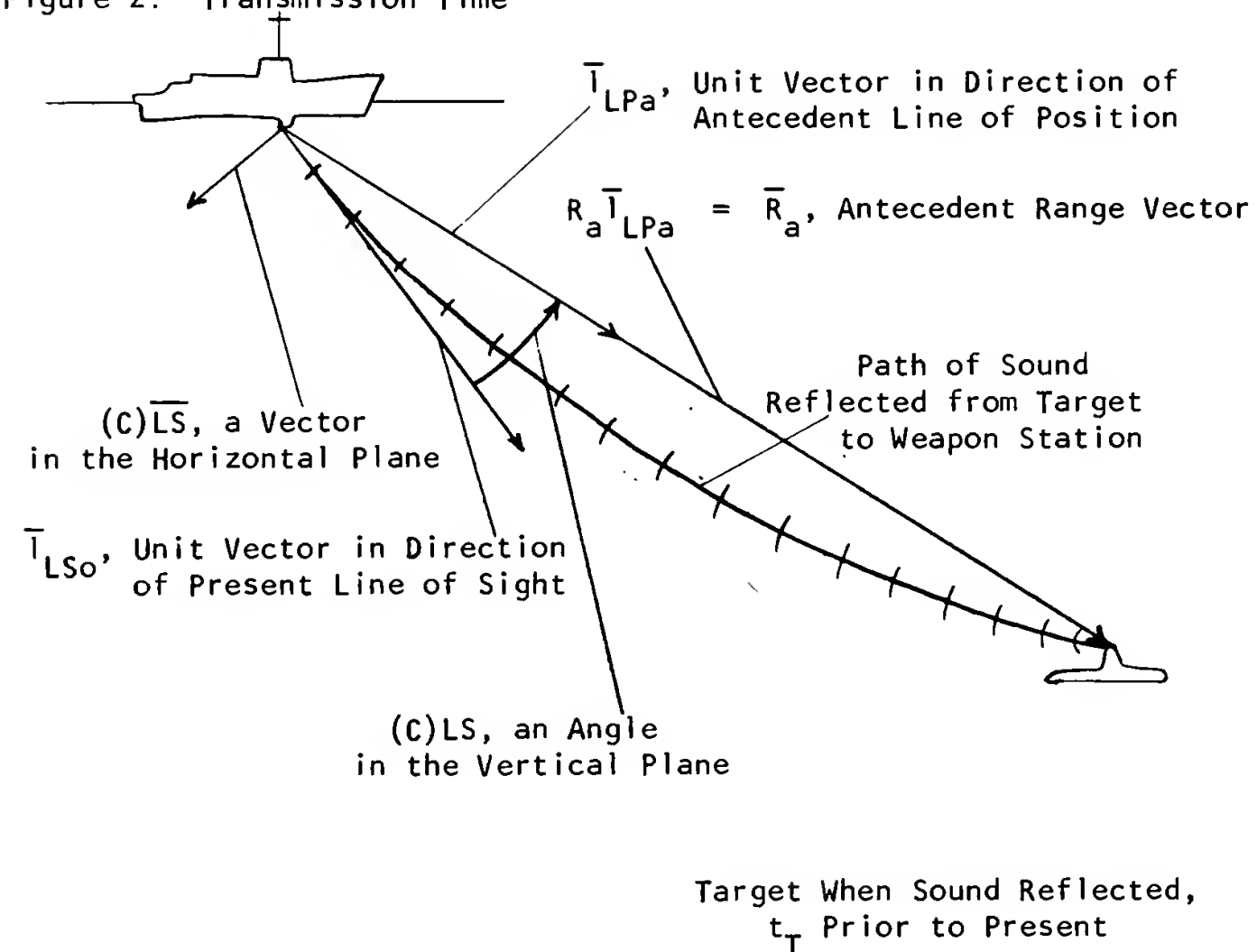
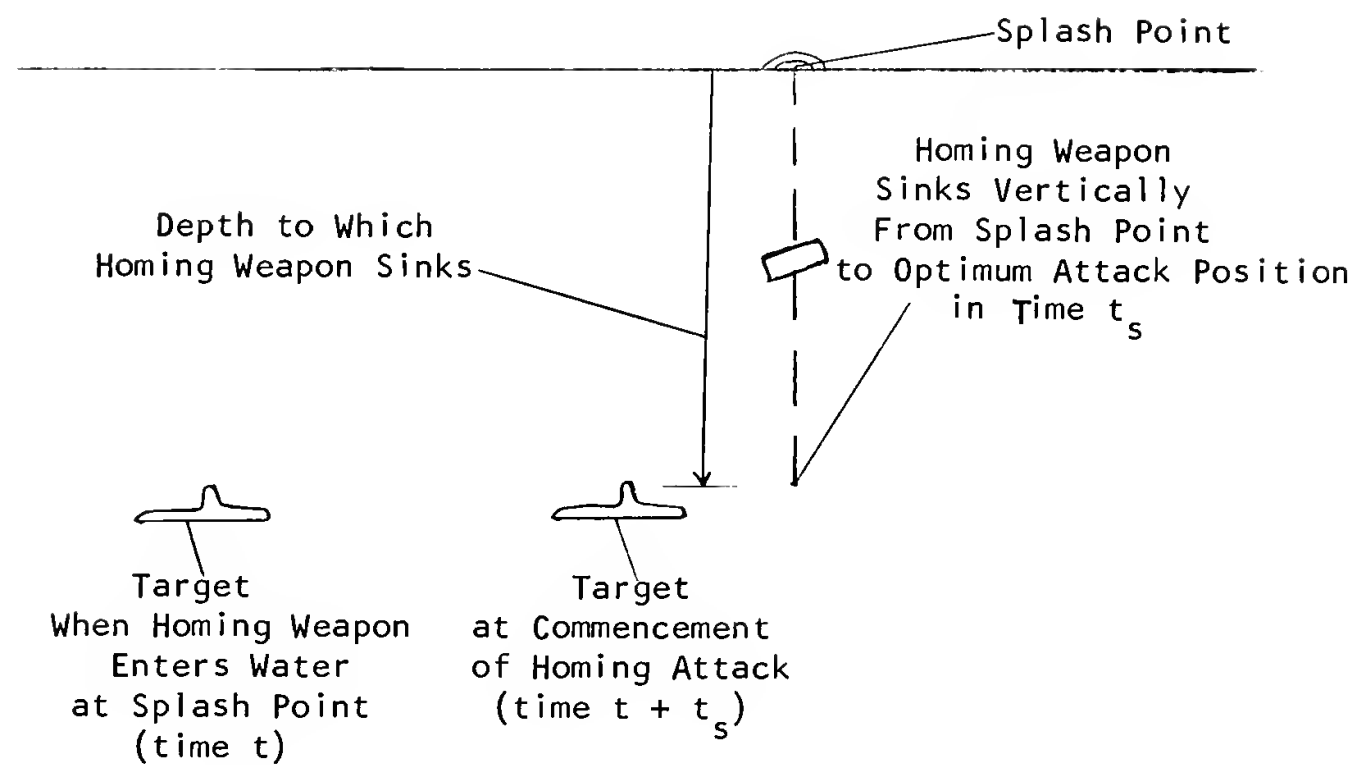
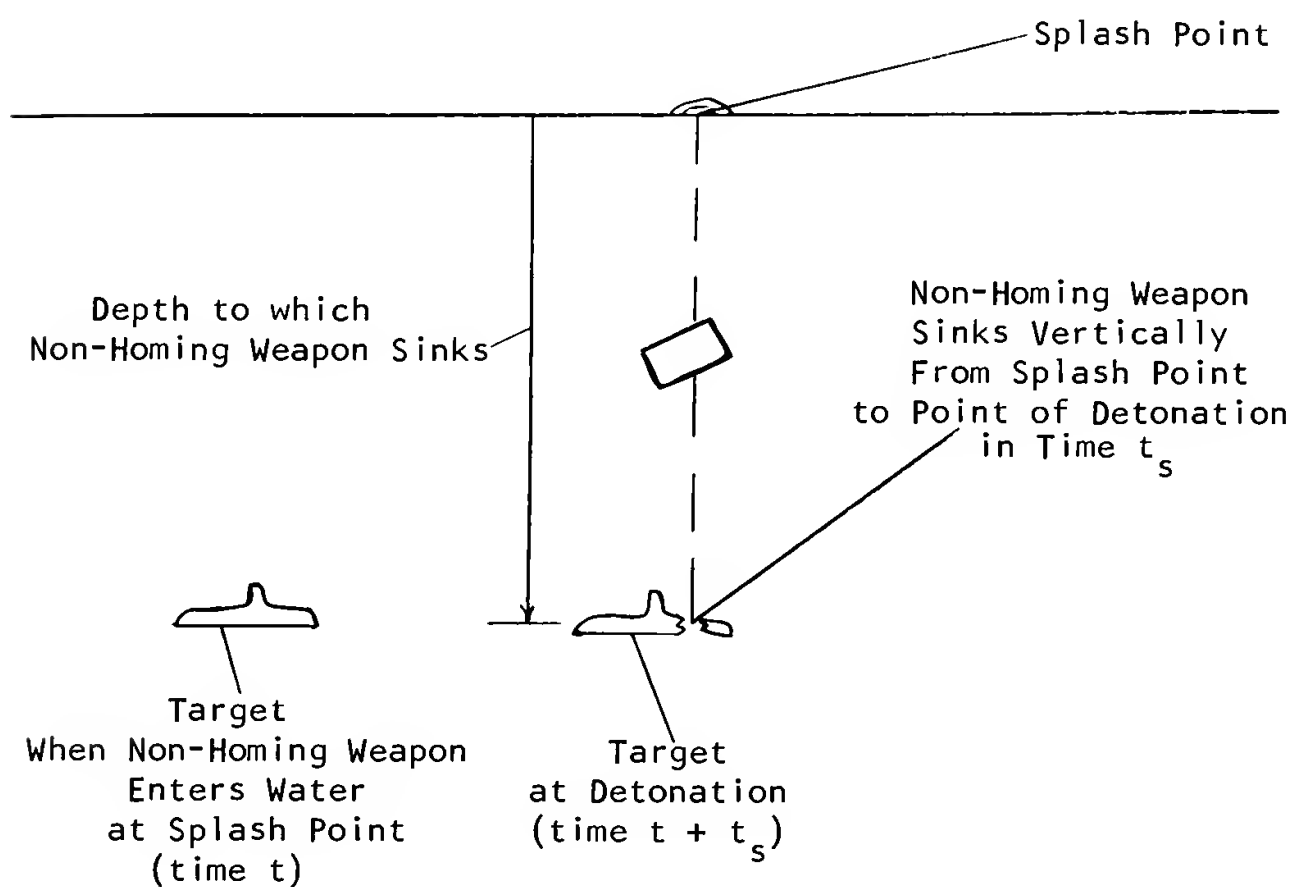


Figure 3. The Relationship Between Line of Sight and Line of Position



a) The Homing Case



b) The Non-Homing Case

Figure 4. Sinking Time

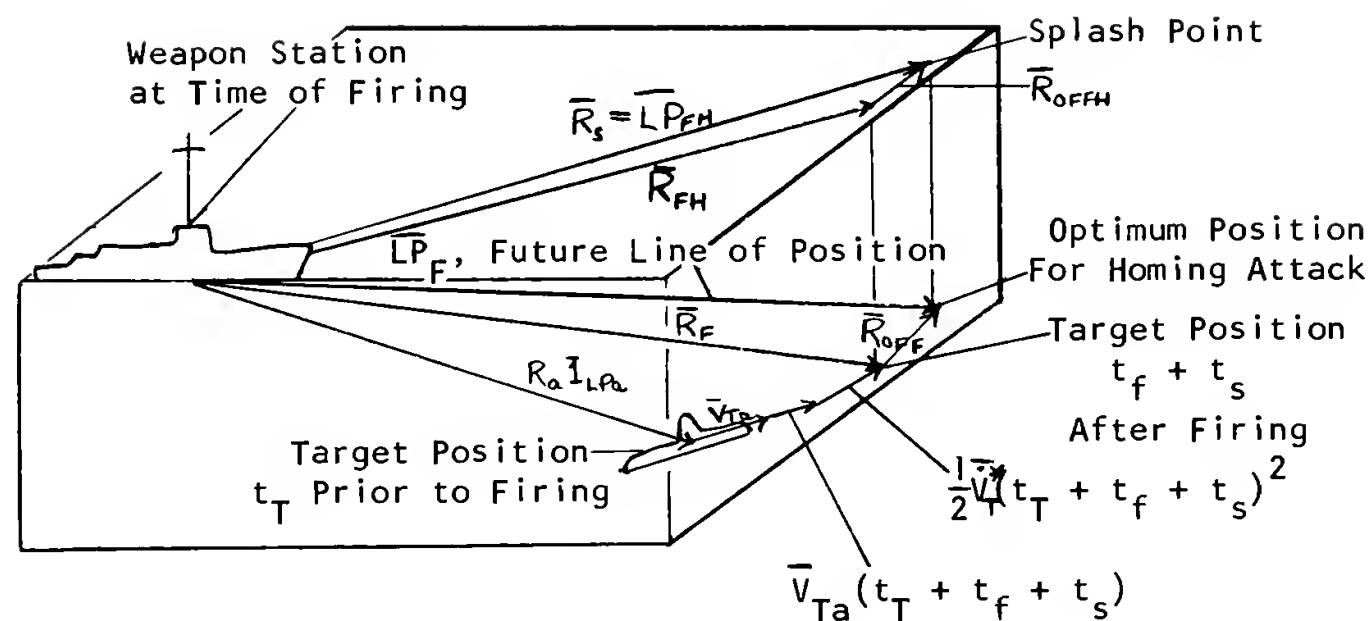


Figure 5. The Relationship of Future Range and Offset Range to Splash Range

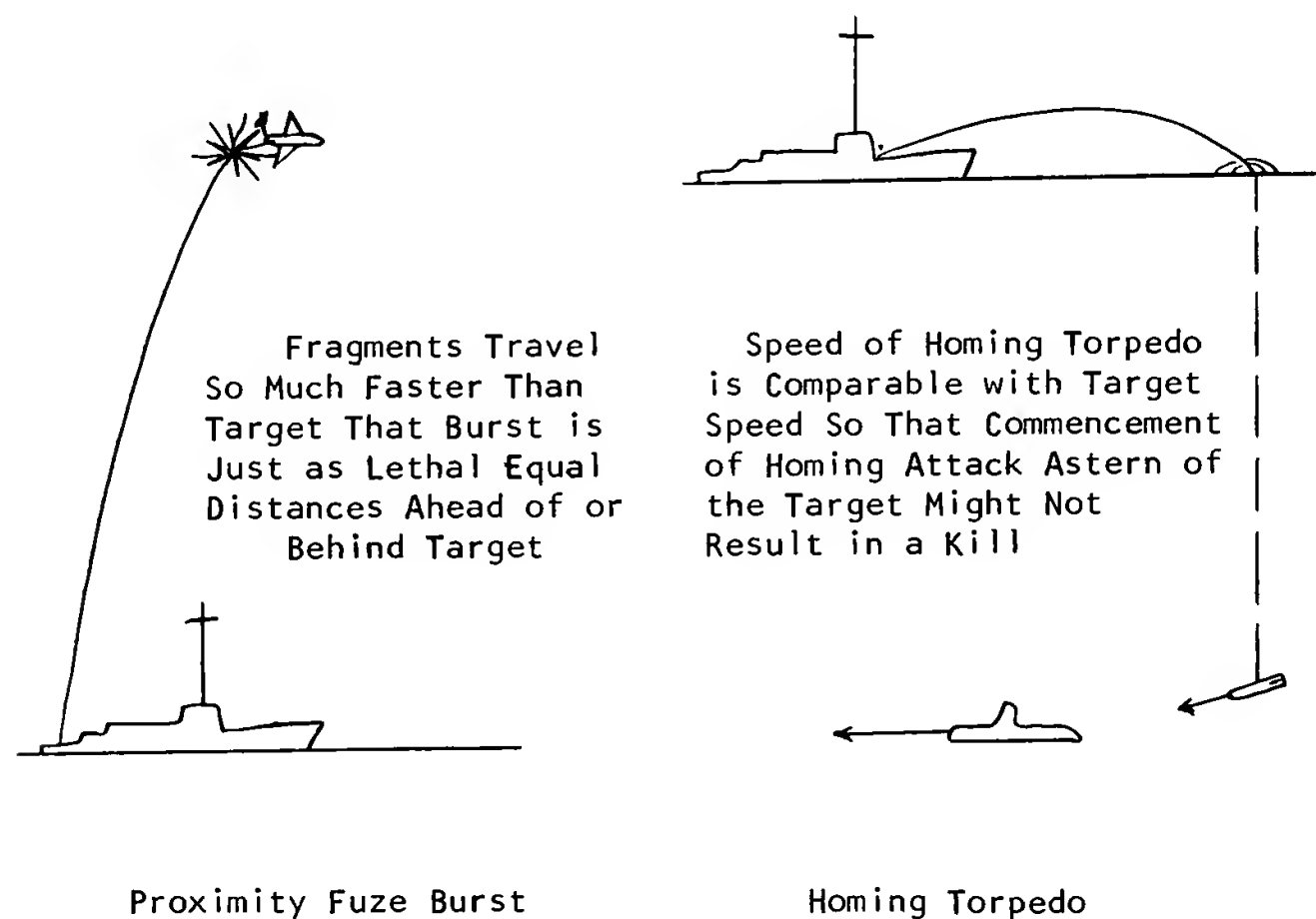


Figure 6. Center of Lethality

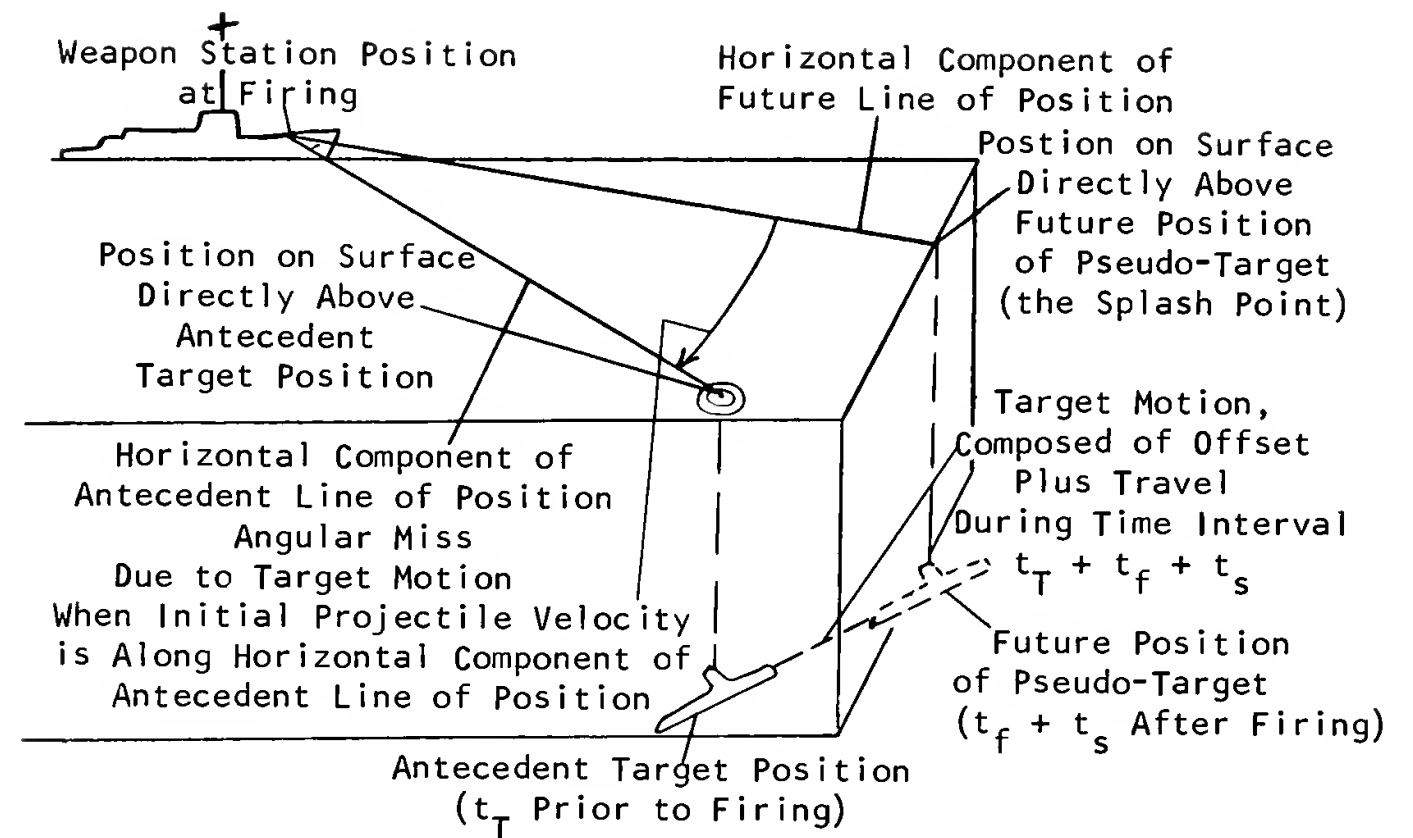


Figure 7. Target Motion as a Miss-Producing Effect

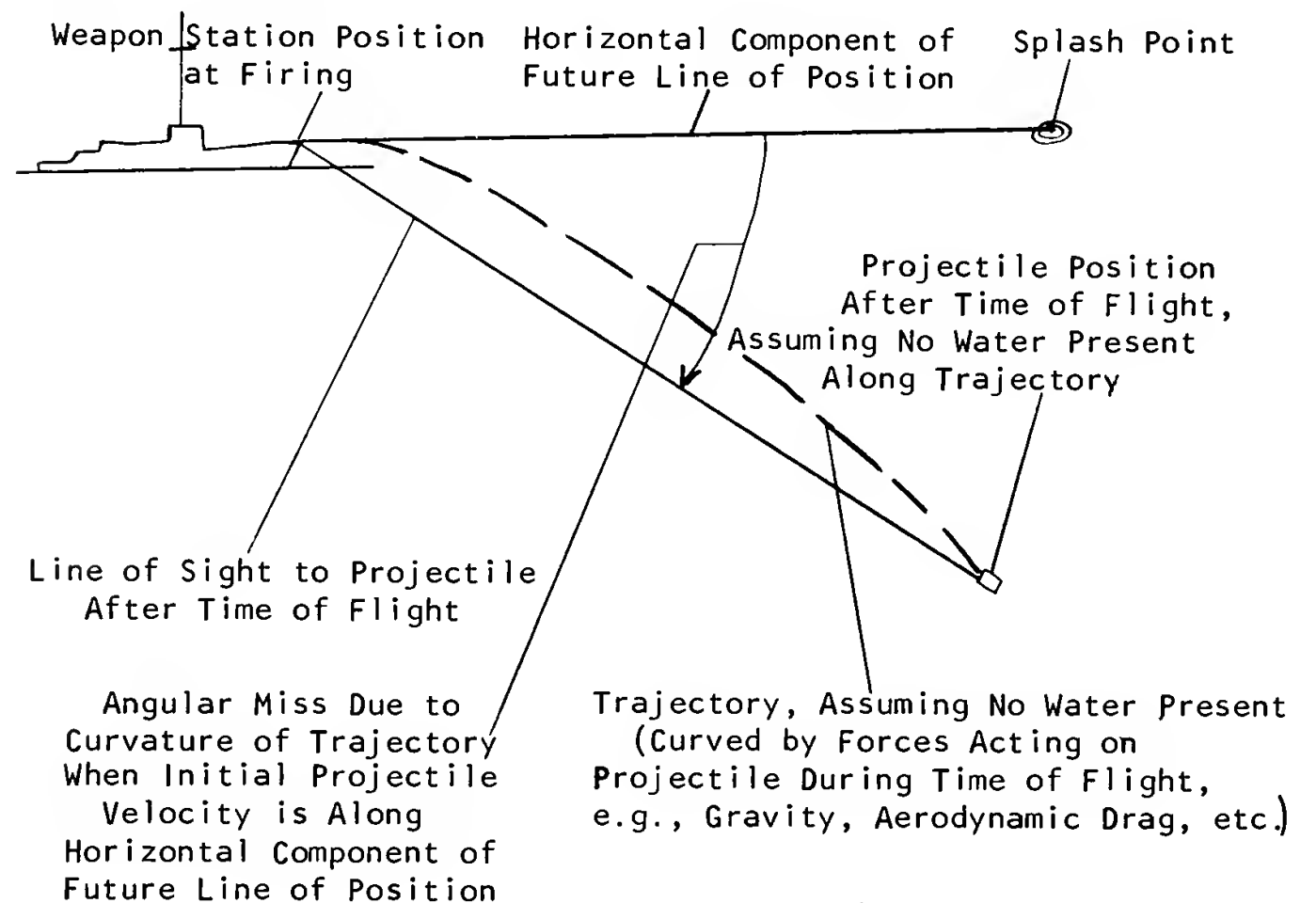


Figure 8. Curvature of the Trajectory as a Miss-Producing Effect

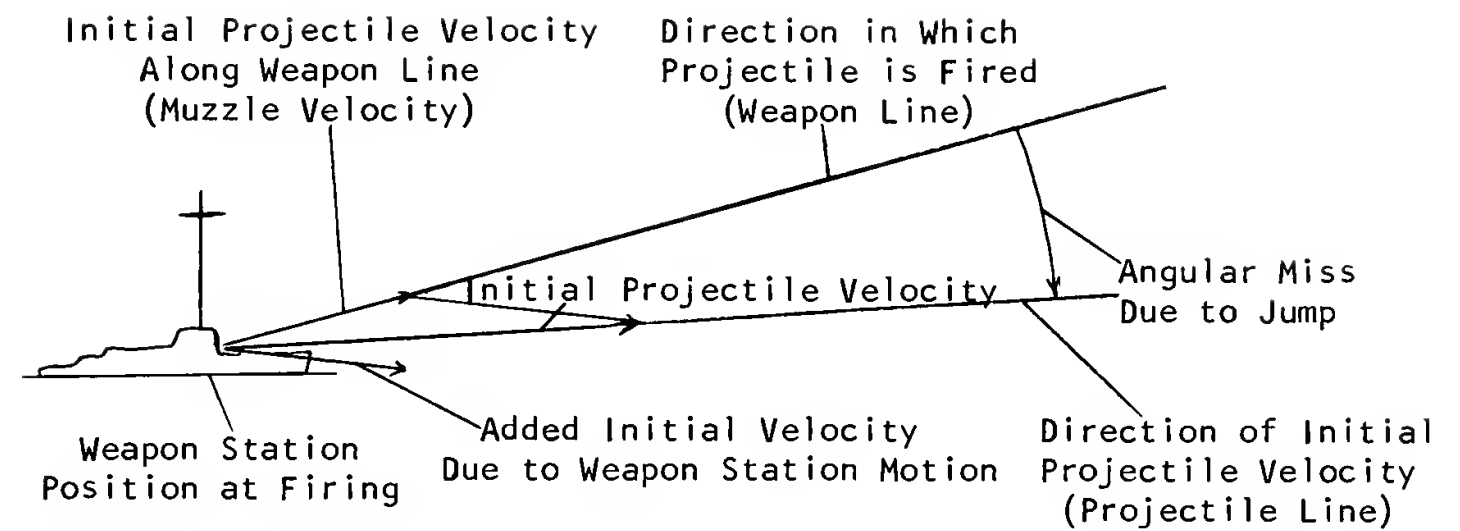


Figure 9. Jump as a Miss-Producing Effect

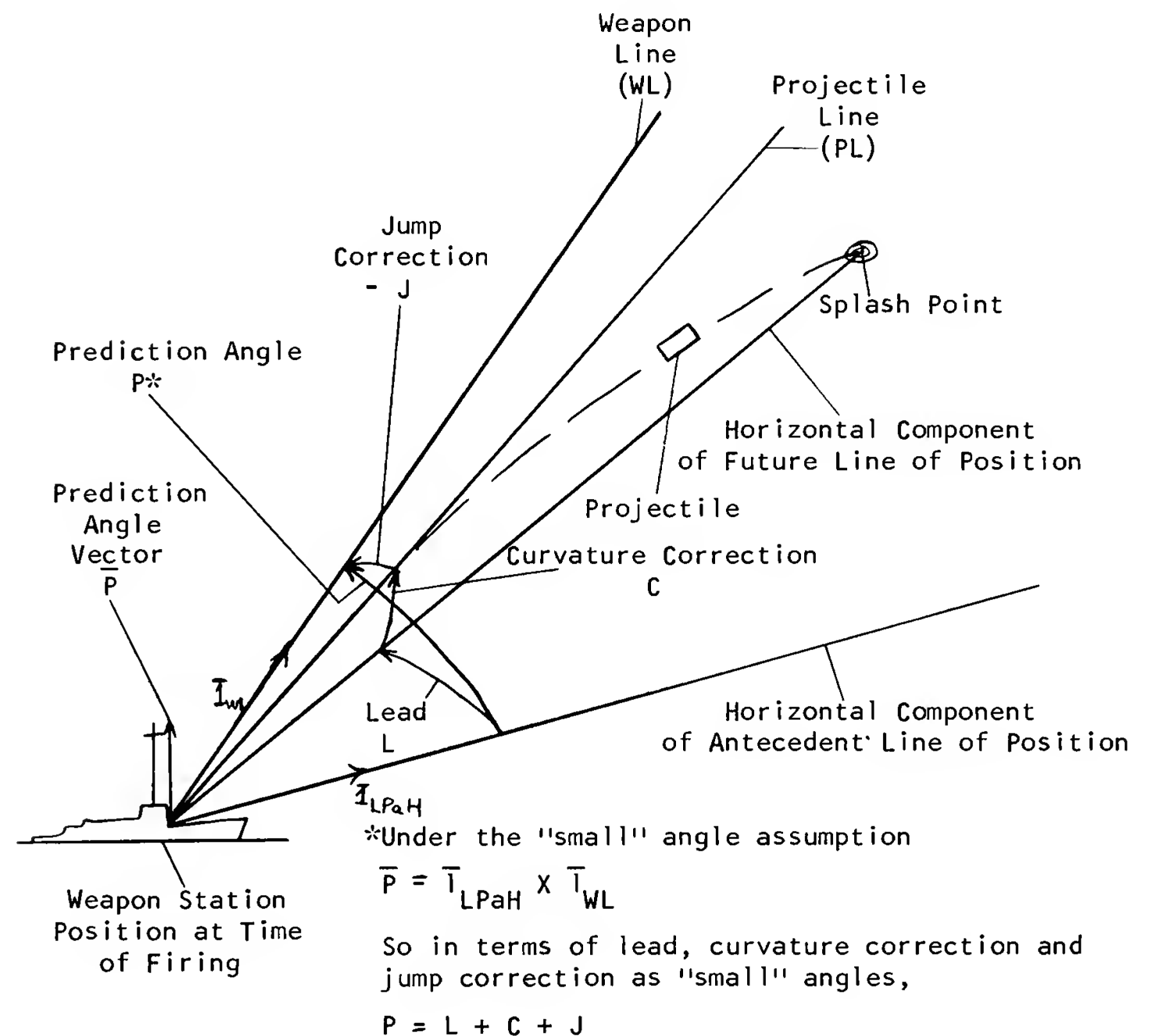


Figure 10. Geometrical Features of the Complete Problem

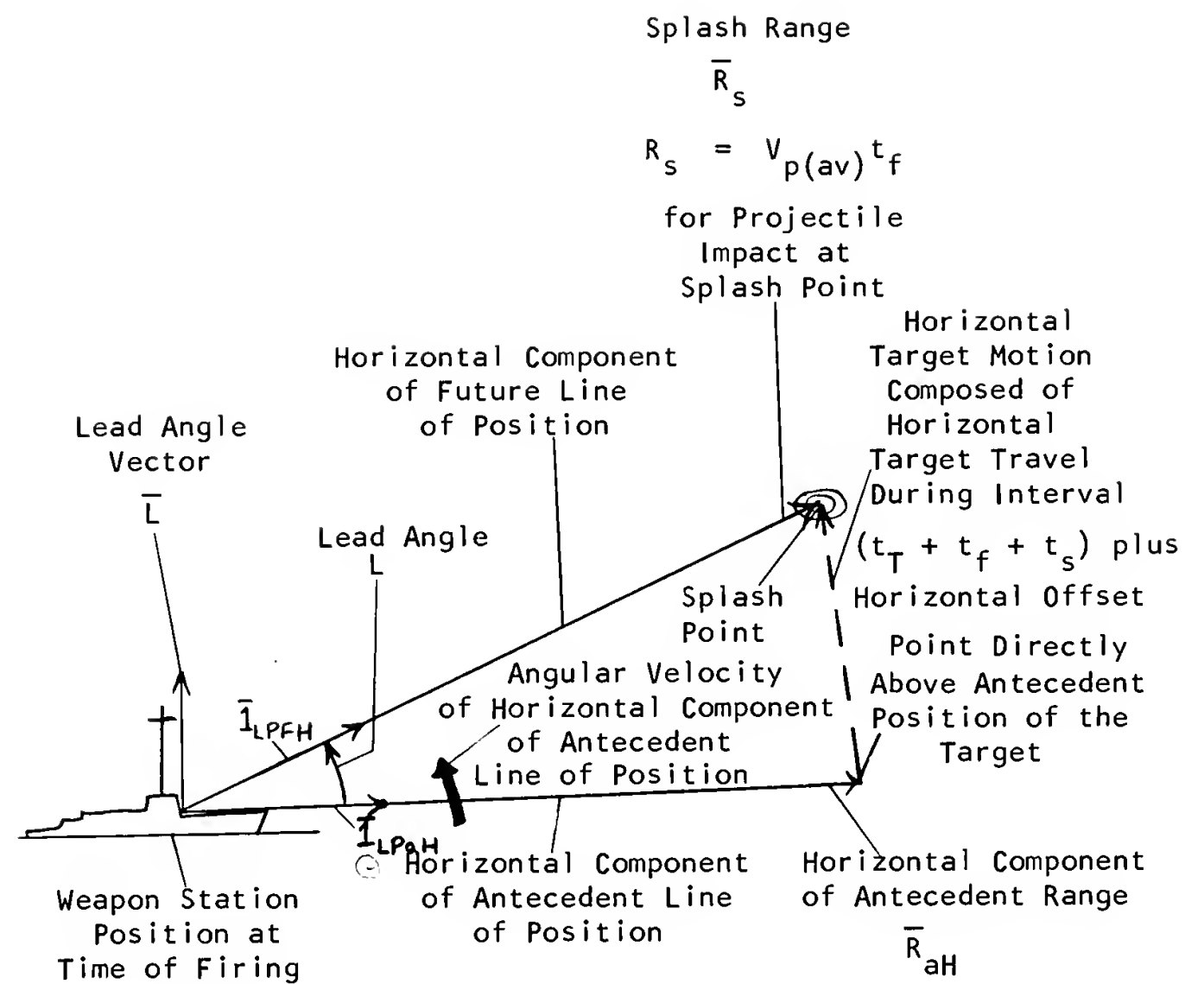


Figure 11. Geometrical Features of Lead Angle

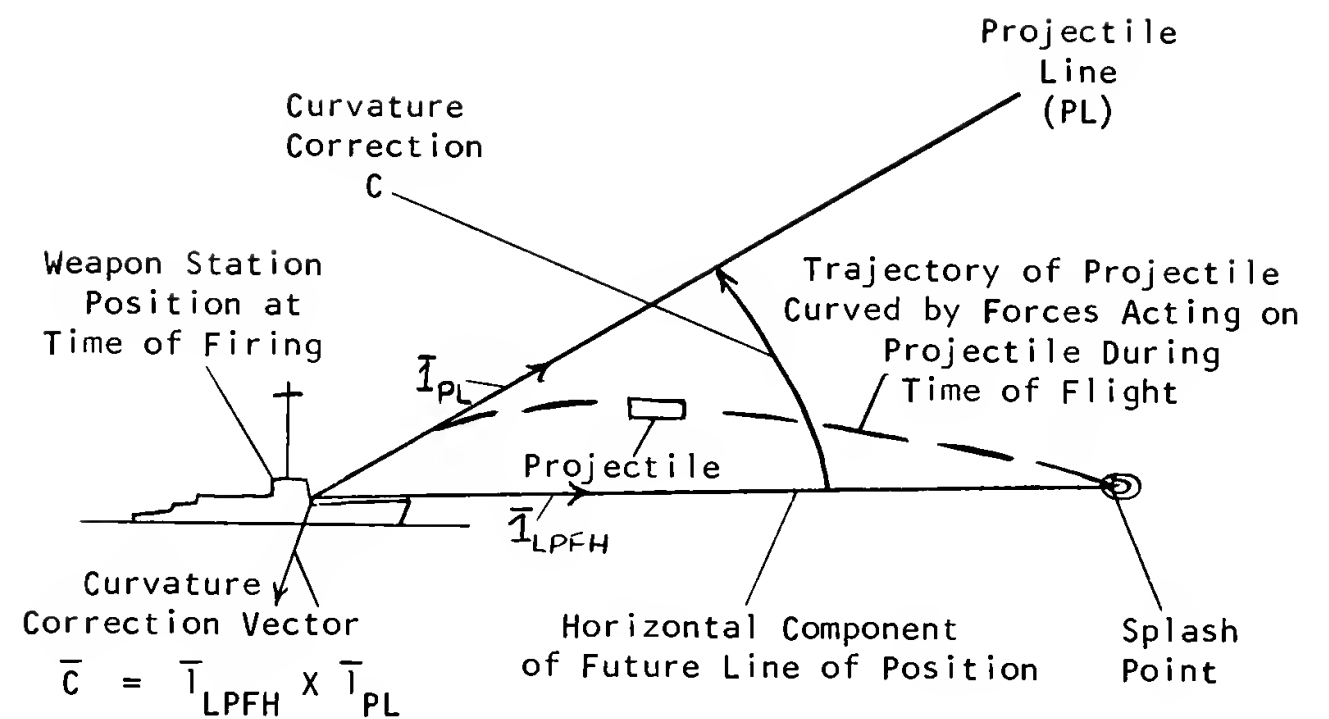


Figure 12. Geometrical Features of Curvature Correction

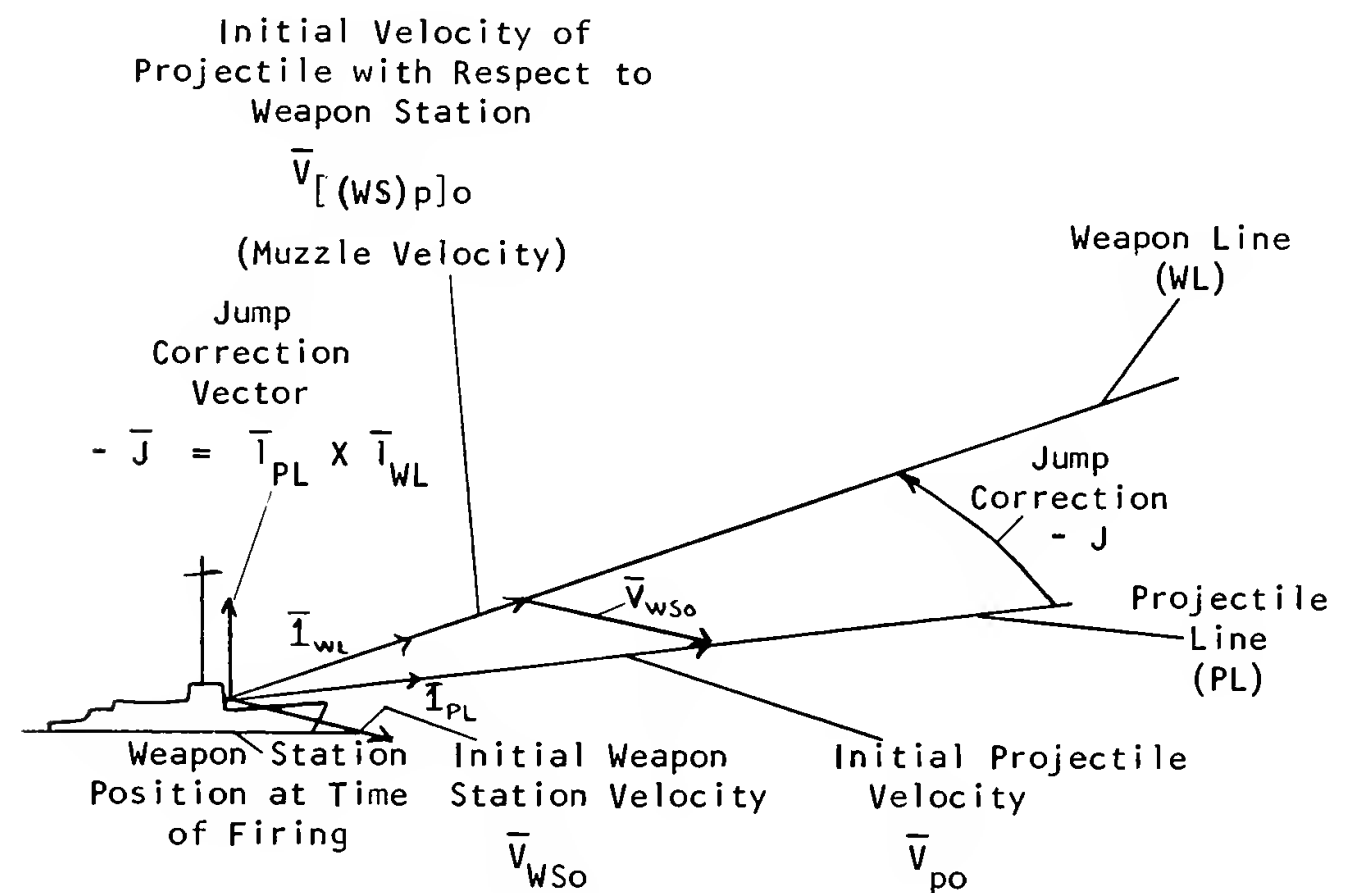
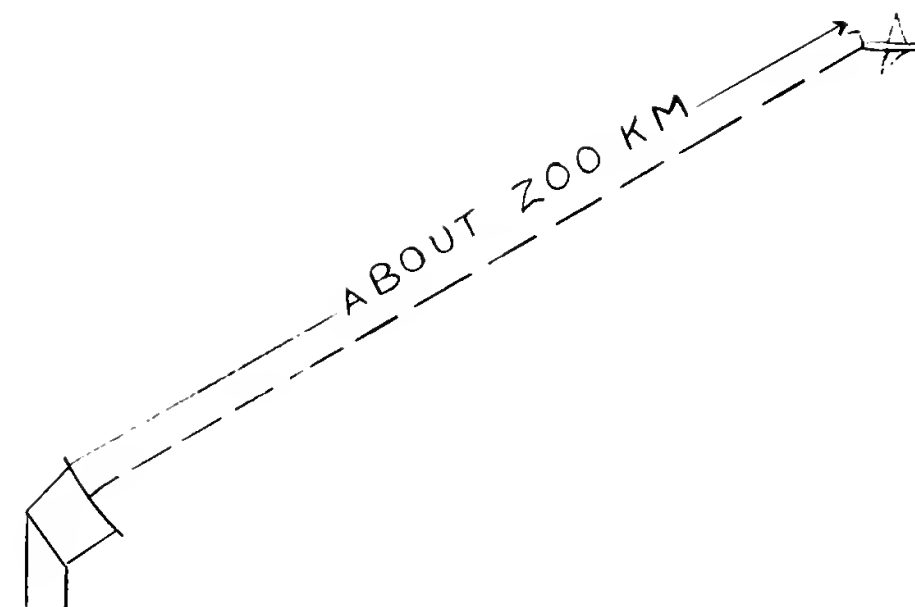
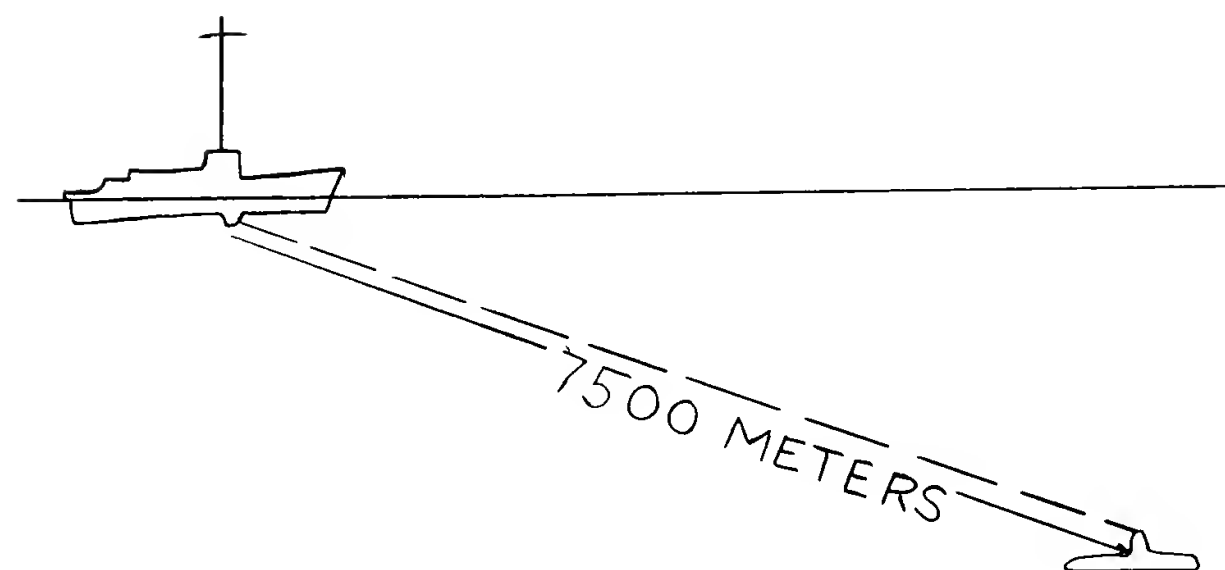


Figure 13. Geometrical Features of Jump Correction



Electromagnetic
Radiation Can Travel
Out to a Target About
200 KM. Away and Return
800 Times a Second



Sound Waves
Require 10 Seconds
to Reach an Underwater
Target 7500 Meters Away
and Return

Figure 14. Information Rates in Electromagnetic and Sound Radiation

$$R_a(t) \bar{i}_{LPa}(t) = R_{ax}(t) \bar{i} + R_{ay}(t) \bar{j} + R_{az}(t) \bar{k}$$

$$\begin{aligned} \bar{R}_{WS} &= \bar{V}_{WS0} \Delta t \\ &= (V_{WSx} \bar{i} + V_{WSy} \bar{j} + 0 \bar{k}) \Delta t \end{aligned}$$

$$\Delta \bar{R}_T = \Delta \bar{R}_{[(WS)T]} + \Delta \bar{R}_{WS}$$

$$\Delta R_{Tx} = R_{ax}(t + \Delta t) - R_{ax}(t) + V_{WSx} \Delta t$$

$$\Delta R_{Ty} = R_{ay}(t + \Delta t) - R_{ay}(t) + V_{WSy} \Delta t$$

$$\Delta R_{Tz} = R_{az}(t + \Delta t) - R_{az}(t)$$

$\Delta \bar{R}_T$

$$\begin{aligned} R_a(t + \Delta t) \bar{i}_{LPa}(t + \Delta t) &= R_{ax}(t + \Delta t) \bar{i} + R_{ay}(t + \Delta t) \bar{j} + \\ &+ R_{az}(t + \Delta t) \bar{k} \end{aligned}$$

$$\bar{V}_{Ta} = V_{TaH} + V_{TaV}$$

$$\bar{V}_{TaH} = \frac{1}{\Delta t} (\Delta R_{Tx} \bar{i} + \Delta R_{Ty} \bar{j})$$

$$\bar{V}_{TaV} = \frac{1}{\Delta t} (\Delta R_{Tz} \bar{k})$$

Figure 15. Determination of \bar{V}_{Ta}

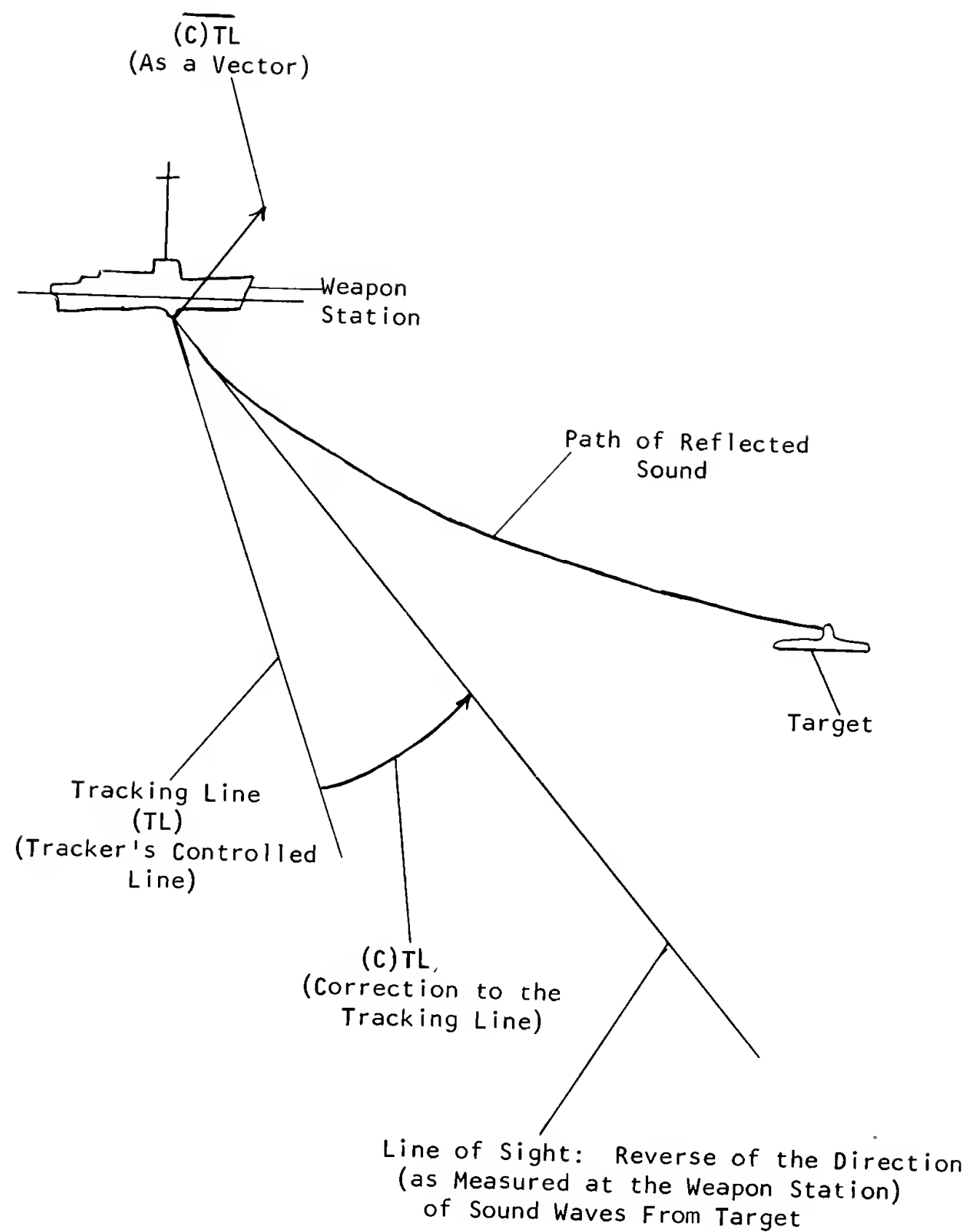
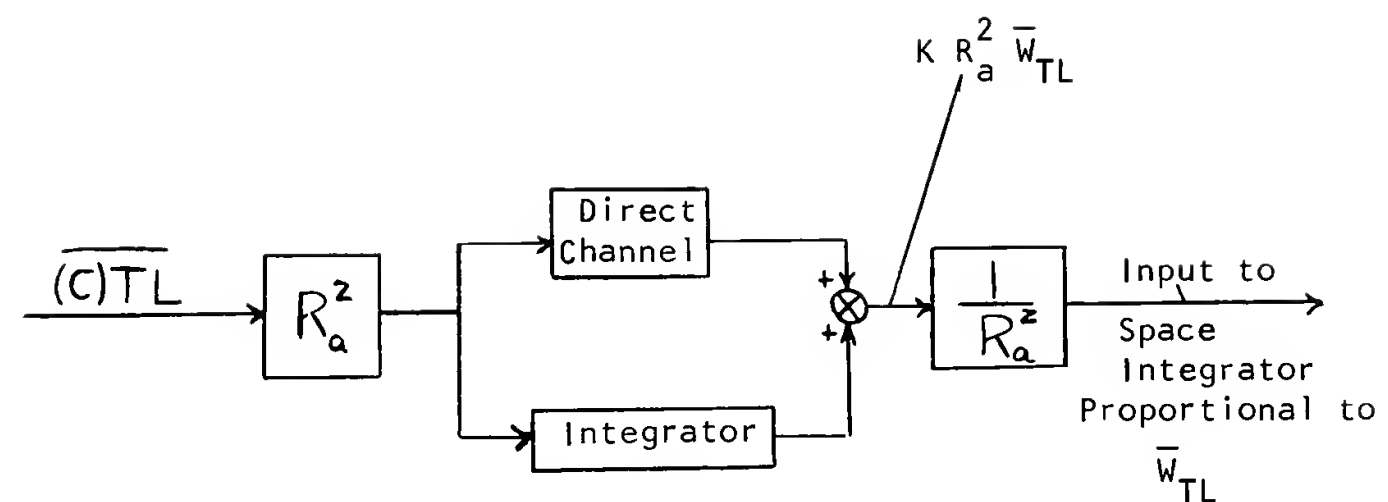


Figure 16. The Geometrical Relationships Between the Line of Sight, the Tracking Line, and the Correction to the Tracking Line



If \bar{V}_{Ta} is constant, $R_a^2 \bar{W}_{LSO}$ is constant. In this case a sketch of a typical time history of various signals is shown below starting from random initial conditions.

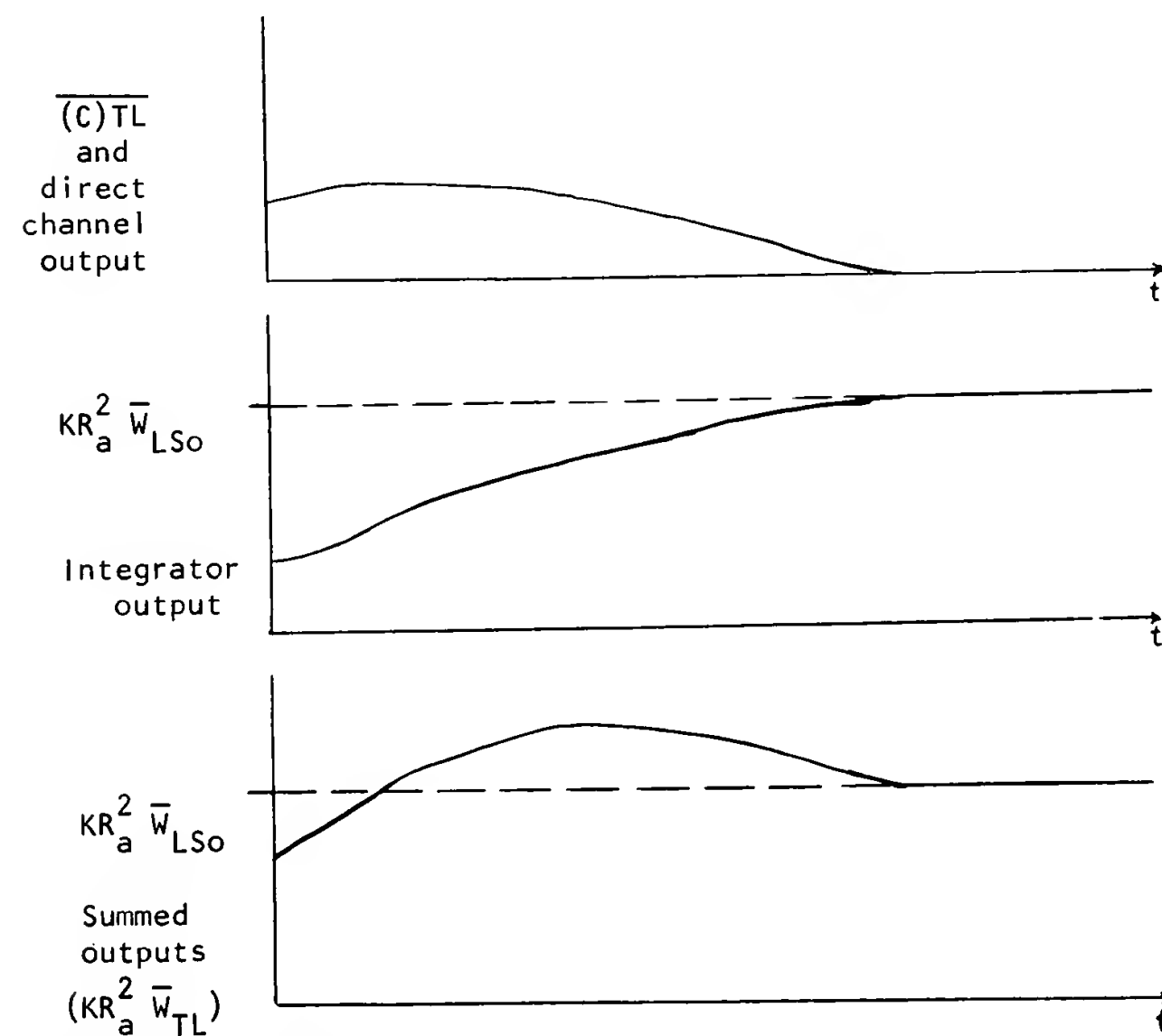


Figure 17. A Signal Modifier for Use with the Controlled Line Method

APPENDIX A

AN EXAMPLE OF TARGET INFORMATION TRANSFORMATION

Consider the situation where the roll angle, θ , the pitch angle ϕ , and the heading, Ψ , of the weapon station are obtained as follows.¹ The origin of the reference coordinate system is fixed in the weapon station and it has x_0 , y_0 , and z_0 axes oriented north, east, and down respectively. The weapon station structure is initially aligned with the reference system. Consider figure A-1. A heading of Ψ aligns the structure with the axis system x_1 , y_1 and z_1 . Note that since heading is measured about the z_0 axis that the z_0 and z_1 axes are coincident.

Pitch angle is measured relative to the x_1 , y_1 , z_1 system and is developed by a rotation of the structure about the y_1 axis into the x_2 , y_2 , z_2 axis system. Note that the y_1 and y_2 axes are coincident.

Finally, from its alignment with the x_2 , y_2 , z_2 axis system, the weapon station structure rolls about the x_2 axis into alignment with the x_3 , y_3 , z_3 axis system. Here the x_2 and x_3 axes are coincident.

¹The sequence used here is employed because a gyrocompass can measure Ψ and because most weapon stations roll to much greater angles than they pitch. This writer has experienced roll angles in excess of 50 degrees in a destroyer.

The weapon station receives target information that can be represented by a vector \bar{R} . Its coordinates are known relative to the weapon station structure, i.e., in the x_3, y_3, z_3 axis system. The transformation to the reference coordinate system of x_0, y_0, z_0 is conceptually done in three steps. Let $[R]_n$ symbolize a column matrix representing the vector \bar{R} coordinatized in the x_n, y_n, z_n axis system.

$$\text{Then } [\bar{R}]_2 = [A][\bar{R}]_3 \quad (A-1)$$

$$[\bar{R}]_1 = [B][\bar{R}]_2 = [B][A][\bar{R}]_3 \quad (A-2)$$

$$[\bar{R}]_0 = [C][\bar{R}]_1 = [C][B][A][\bar{R}]_3 \quad (A-3)$$

It can be seen from figure A-1 that

$$[A] = \begin{bmatrix} 1 & 0 & 0 \\ 0 & \cos \theta & \sin \theta \\ 0 & -\sin \theta & \cos \theta \end{bmatrix} \quad (A-4)$$

$$[B] = \begin{bmatrix} \cos \phi & 0 & \sin \phi \\ 0 & 1 & 0 \\ -\sin \phi & 0 & \cos \phi \end{bmatrix} \quad (A-5)$$

$$[C] = \begin{bmatrix} \cos \psi & \sin \psi & 0 \\ -\sin \psi & \cos \psi & 0 \\ 0 & 0 & 1 \end{bmatrix} \quad (A-6)$$

By matrix multiplication

$$[C][B] = \begin{bmatrix} \cos\phi\cos\psi & \sin\psi & \sin\phi\cos\psi \\ -\cos\phi\sin\psi & \cos\psi & -\sin\phi\sin\psi \\ -\sin\phi & 0 & \cos\phi \end{bmatrix} \quad (A-7)$$

$$[C][B][A] =$$

$$\begin{bmatrix} \cos\phi\cos\psi & \cos\phi\sin\psi - \sin\theta\sin\phi\cos\psi & \sin\theta\sin\psi + \cos\theta\sin\phi\cos\psi \\ -\cos\phi\sin\psi & \cos\phi\cos\psi + \sin\theta\sin\phi\sin\psi & \sin\theta\cos\psi - \cos\theta\sin\phi\sin\psi \\ -\sin\phi & -\sin\theta\cos\phi & \cos\theta\cos\phi \end{bmatrix} \quad (A-8)$$

Employing the transformation matrix of equation (A-8), target information is transformed from the axis system of the weapon station structure into the reference coordinate system. The reference coordinate system of this example is the same as the water-mass frame for coordinatizing position vectors. Since the weapon station is moving relative to the water-mass, this is not so for velocity vectors. However, the target information available is all position data, so the transformation of equation (A-8) gives this information coordinatized in the water-mass frame.

From initial alignment in the x_0, y_0, z_0 frame, the weapon station structure is carried into the x_1, y_1, z_1 frame by heading, ψ , thence into the x_2, y_2, z_2 frame by pitch, ϕ , and finally into the x_3, y_3, z_3 frame by roll, θ .

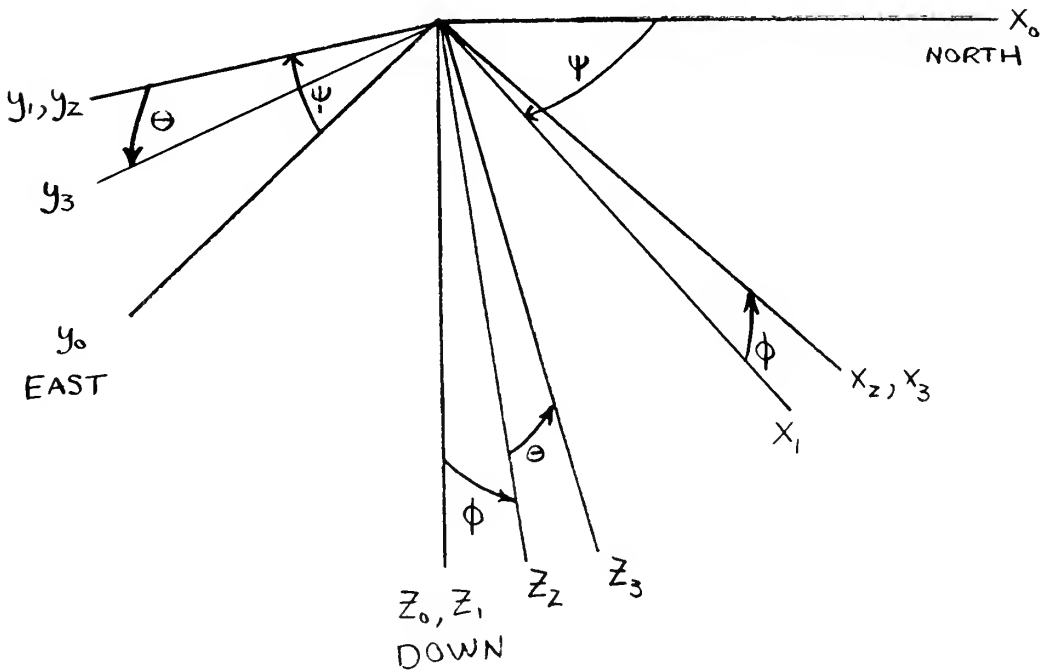


Figure A-1 Axis Systems in Weapon Station Structure Angular Motion

REFERENCES

- (1) Thach, J. W., "The ASW Navy of the Seventies," U.S. Naval Institute Proceedings, LXXXIX, January 1963.
- (2) Wrigley, W. and Hovorka, J., Fire Control Principles, McGraw-Hill Book Company, Inc., New York, 1959.
- (3) Messere, E. R., The Principles of Submarine Torpedo Fire Control, Massachusetts Institute of Technology Master of Science Thesis, Instrumentation Laboratory Report T-382, Cambridge, Mass., May 1964.
- (4) Kinsler, L. E., and Frey, A. R., Fundamentals of Acoustics, John Wiley and Sons, Inc., New York, 1950.
- (5) Cockaday, L. M., Daley, J. L., and Leydorf, G. E., Basic Course in Electronics, 2d ed., U. S. Naval Institute, Annapolis, Maryland, 1950.
- (6) Draper, C. S., Wrigley, W., and Grohe, L. R., The Floating Integrating Gyro And Its Application to Geometrical Stabilization Problems on Moving Bases, S.M.F. Fund Paper No. FF-13, Institute of the Aeronautical Sciences, New York, January 1955.
- (7) Markey, W. R., The Effect of System Configuration on Fire Control Performance, Massachusetts Institute of Technology Doctor of Science Thesis, Instrumentation Laboratory Report T-65, Cambridge, Mass., May 1956.

thesB726

An investigation of the surface-to-under



3 2768 002 07327 2
DUDLEY KNOX LIBRARY